

# Momentum-driven feedback and the $M$ – $\sigma$ relation in non-isothermal galaxies

Rachael C. McQuillin\* and Dean E. McLaughlin

*Astrophysics Group, Lennard Jones Laboratories, Keele University, Keele, Staffordshire, ST5 5BG, UK*

21 August 2018

## ABSTRACT

We solve for the velocity fields of momentum-conserving supershells driven from galaxy centres by steady winds from supermassive black holes or nuclear star clusters (central massive objects: CMOs). We look for the critical CMO mass that allows such a shell to escape from its host galaxy. In the case that the host galaxy dark matter halo is a singular isothermal sphere, we find that the critical CMO mass derived by King, which scales with the halo velocity dispersion as  $M_{\text{crit}} \propto \sigma^4$ , is necessary, but not by itself sufficient, to drive shells to large radii in the halo. Furthermore, a CMO mass at least 3 times the King value is required to drive the shell to the escape speed of the halo. In the case of CMOs embedded in protogalaxies with non-isothermal dark matter haloes, which we treat here for the first time, we find a critical CMO mass that *is sufficient* to drive *any* shell (under a steady wind) to escape *any* galaxy with a peaked circular speed profile. In the limit of large halo mass, relevant to real galaxies, this critical CMO mass depends only on the value of the peak circular speed of the halo, scaling as  $M_{\text{crit}} \propto V_{\text{c,pk}}^4$ . Our results therefore relate to observational scalings between black hole mass and asymptotic circular speed in galaxy spheroids. They also suggest a natural way of extending analyses of  $M$ – $\sigma$  relations for black holes in massive bulges, to include similar relations for nuclear clusters in lower-mass and disc galaxies.

**Key words:** galaxies: nuclei — galaxies: formation — galaxies: evolution

## 1 INTRODUCTION

Most early-type galaxies and bulges with  $M \gtrsim 10^{10} M_{\odot}$  harbour a supermassive black hole (SMBH) at their centre (Kormendy & Richstone 1995); while observations with the *Hubble Space Telescope* have revealed the presence of massive nuclear star clusters (NCs) in the majority of less massive galaxies (both early- and late-type: Phillips et al. 1996; Carollo et al. 1997; Böker et al. 2002; Côté et al. 2006, 2007). The properties of these central massive objects (CMOs) correlate tightly with properties of their host galaxies, perhaps most notably in terms of CMO mass,  $M_{\text{CMO}}$ , versus (bulge) stellar velocity dispersion,  $\sigma$ :  $M_{\text{CMO}} \propto \sigma^x$ , with  $x \simeq 4$  (for SMBHs, see, e.g., Ferrarese & Merritt 2000, Gebhardt et al. 2000, Tremaine et al. 2002, Ferrarese & Ford 2005, or Gültekin et al. 2009; for NCs, see Ferrarese et al. 2006; also relevant are Wehner & Harris 2006 and Rossa et al. 2006). Though essentially parallel, there is an offset between the  $M$ – $\sigma$  relations of NCs and SMBHs, in the sense that the NC masses in intermediate- and low-mass galaxies tend to be  $\sim 10\times$  larger than if they followed a simple extrapolation

of the SMBH  $M$ – $\sigma$  relation for higher-mass spheroids (Ferrarese et al. 2006; see also McLaughlin et al. 2006).

Recently, Volonteri, Natarajan, & Gültekin (2011; cf. Ferrarese 2002) have argued that galaxies/bulges containing SMBHs also show a correlation, of the form  $M_{\text{bh}} \propto V_{\text{c}}^y$  with  $y \approx 4$ , between black hole mass and the “asymptotic” circular speed  $V_{\text{c}}$  at large radii where dark matter is expected to dominate the total galaxy mass. There is some debate (e.g., see Ho 2007; Kormendy & Bender 2011) over how the stellar velocity dispersions in the  $M$ – $\sigma$  relation, which are measured inside a fraction of the bulge effective radius, connect *empirically* to asymptotic circular speeds, which normally refer to many times the effective radius defined by stars. This can be a difficult question (with a model-dependent answer), especially in “hot” stellar systems where circular speeds—that is,  $V_{\text{c}}^2(r) = GM(r)/r$ —are not observed simply as net rotation. However, the existence of *some* kind of connection, and at least the possibility of an  $M_{\text{bh}}$ – $V_{\text{c}}$  relation in addition to  $M_{\text{bh}}$ – $\sigma$ , is clear in principle: The stellar velocity dispersion at *any* radius in a dark-matter dominated galaxy depends on the dark matter distribution, which is precisely what  $V_{\text{c}}$  probes at large radii.

Self-regulated feedback from growing CMOs is thought

\* E-mail: rcm@astro.keele.ac.uk

to play a key role in establishing the  $M$ - $\sigma$  relation and associated scalings. Though through different mechanisms, either an NC or an SMBH will drive an outflow, which sweeps the ambient gas in a protogalaxy into a shell that, at least initially, is able to cool rapidly and is therefore momentum-driven (King 2003; McLaughlin et al. 2006; see also §2 below). There is then a critical CMO mass above which the outwards force of the wind on the shell may overcome the inwards gravitational pull of the CMO plus the dark matter halo of the parent galaxy.

The only case that has been considered in detail analytically is that of a steady wind, in which the CMO mass (and associated wind thrust) is constant throughout the motion of the shell (Silk & Rees 1998; Fabian 1999; King 2003, 2005, 2010a; Murray et al. 2005; McLaughlin et al. 2006; Silk & Nusser 2010). In this case, *and* assuming a halo modelled as a singular isothermal sphere (SIS) with velocity dispersion  $\sigma_0$ , King (2005) found a critical CMO mass of

$$M_{\text{crit}} = \frac{f_0 \kappa}{\lambda \pi G^2} \sigma_0^4 \simeq 4.56 \times 10^8 M_\odot \sigma_{200}^4 f_{0.2} \lambda^{-1}, \quad (1)$$

(see also McLaughlin et al. 2006; Murray et al. 2005). In this expression,  $\kappa = 0.398 \text{ cm}^2 \text{ g}^{-1}$  is the electron scattering opacity;  $f_0$  is an average gas mass fraction ( $\approx 0.2$ , so  $f_{0.2} = f_0/0.2$ ); and  $\sigma_{200} = \sigma_0/200 \text{ km s}^{-1}$ . The parameter  $\lambda$  is related to the feedback efficiency for each type of CMO; it has a value  $\lambda \approx 1$  for SMBHs, and  $\lambda \approx 0.05$  for NCs (McLaughlin et al. 2006). Once a CMO in an isothermal halo with a given  $\sigma_0$  has grown to at least the mass in equation (1), the CMO wind may drive a momentum-conserving shell with coasting speed  $v > 0$  at arbitrarily large radii in the galaxy. This then admits the possibility of a blow-out clearing the galaxy of any remaining ambient gas, choking off further star formation and CMO growth, and locking in an  $M_{\text{CMO}}-\sigma$  relation.

As a momentum-driven shell moves outwards from a CMO, gas cooling times increase and a switch to an energy-driven phase is expected, at which point the shell can accelerate to escape the galaxy (King 2003). Momentum-driving may then need only push a shell out to where the switch to energy-driving occurs; and this can be done with a CMO less massive than the  $M_{\text{crit}}$  in equation (1), which is necessary for momentum-driving to *arbitrarily* large radii. This suggests that equation (1) may actually predict an upper limit for observed  $M$ - $\sigma$  relations; and indeed, the equation lies above current best fits to data by factors of a few.

Distributed star formation in a protogalaxy bulge is expected to provide additional momentum input to the feedback (Murray et al. 2005; Power et al. 2011). This would also reduce the CMO mass required for the feedback to escape, again suggesting that the  $M_{\text{CMO}}-\sigma$  relation in equation (1) is an upper limit.

Silk & Nusser (2010) have shown that, in a truncated isothermal sphere specifically, a momentum-conserving shell driven solely by a steady black-hole wind can reach large radius with fast enough speed to escape directly (that is, with  $v \gtrsim 2\sigma_0$ ), only if the SMBH mass is at least a few times *larger* than the critical value in equation (1) (which is necessary just to have  $v > 0$  at large  $r$ ). This would put the predicted normalization of an  $M_{\text{CMO}}-\sigma$  relation above the observed normalization by a full order of magnitude. Silk & Nusser argue from this that the real key to a feedback origin

for  $M_{\text{CMO}}-\sigma$  is momentum input from distributed bulge-star formation that is triggered by the outflow from a CMO. However, Power et al. (2011) counter that a switch from momentum- to energy-driving of the CMO feedback is still inevitable and will alleviate some of the difficulty identified by Silk & Nusser.

In this paper, we investigate how this basic feedback scenario for  $M$ - $\sigma$  relations depends on the simplifying assumption that dark matter haloes are SISs. We analyze aspects of the dynamics of supershells in spherical but non-isothermal haloes, while retaining some other simplifying assumptions (steady winds and purely momentum-driven shells) in common with previous work.

Our main result is a generalization of the critical CMO mass that suffices to blow momentum-driven feedback entirely out of *any* realistic, non-isothermal dark matter halo that has a *well-defined maximum in its circular speed profile*,  $V_c^2(r) = GM_{\text{DM}}(r)/r$ . For large halo masses, this critical CMO mass tends to the limiting value,

$$\begin{aligned} M_{\text{crit}} &\longrightarrow \frac{f_0 \kappa}{\lambda \pi G^2} \frac{V_{\text{c,pk}}^4}{4} \\ &= 1.14 \times 10^8 M_\odot \left( \frac{V_{\text{c,pk}}}{200 \text{ km s}^{-1}} \right)^4 f_{0.2} \lambda^{-1}, \quad (2) \end{aligned}$$

where  $V_{\text{c,pk}}$  is the peak value of the circular speed.

In a SIS, which has a constant  $V_c = \sqrt{2}\sigma_0$ , our new equation (2) clearly reduces to equation (1). However—as we discuss in detail in §3 and §4.1 below—in an *isothermal* halo this  $M_{\text{crit}}$  is *necessary but not sufficient*, in general, to guarantee the escape of a momentum-driven CMO wind. By contrast, in the more realistic, *non-isothermal* cases that we consider, equation (2) gives the  $M_{\text{CMO}}$  that is *sufficient* for the escape of any such feedback.

Any momentum-conserving shell driven by a steady wind from a CMO with the mass in equation (2) will eventually accelerate at large radii and exceed the escape speed of any non-isothermal halo with a peaked  $V_c(r)$  profile, even without a possible change to energy-driving, additional momentum feedback from star formation or growth of the CMO (none of which we include in our analysis). Thus, the objection of Silk & Nusser (2010) to equation (1) as the basis for observed  $M$ - $\sigma$  relations applies *only* if dark matter haloes are strictly isothermal.

Equation (2) defines the “characteristic” velocity dispersion that needs to be considered when interpreting observed  $M_{\text{CMO}}-\sigma$  relations in non-isothermal galaxies:  $\sigma_0 \equiv V_{\text{c,pk}}/\sqrt{2}$ . It also gives the first direct, quantitative prediction of an  $M_{\text{CMO}}-V_c$  relation such as that discussed by Volonteri et al. (2011). The result may still be an upper limit to observed relations since we do not consider any transition to energy-conserving feedback, nor any sources of feedback other than steady CMO winds, in this paper.

We begin in §2 by looking at the general equation of motion of a momentum-driven shell as it moves out into a gaseous protogalaxy. In §3 we develop, in more detail than before, the case of the SIS. In §4.1, we analyze the motion of a momentum-driven shell in a general, non-isothermal halo with a peaked circular-speed curve, and derive equation (2). In the rest of §4, we illustrate our general results using three particular dark-matter halo models as examples (those of Hernquist 1990; Navarro, Frenk, & White 1996, 1997; and

Dehnen & McLaughlin 2005). In §5 we summarize the paper and give a brief discussion.

## 2 EQUATION OF MOTION

An SMBH accreting at near- or super-Eddington rates in a gaseous protogalaxy is expected to drive a fast wind back into the galaxy (King & Pounds 2003), with quasi-spherical (i.e., *not* highly collimated) geometries indicated by observations of strong outflows from local AGN (e.g., Tombesi et al. 2010). Similarly, the combined winds and supernovae from massive stars in a very young (still forming) NC will drive a superwind into its host protogalaxy. In a spherical approximation to either case, the wind sweeps up the surrounding ambient gas into a shell. The material in this shell is hot and tries to expand both backwards and forwards, giving rise to two shock fronts, one propagating forwards into the ambient medium and one backwards into the wind. Initially, the shocked wind region can cool efficiently, by inverse Compton scattering for SMBHs (King 2003) and by atomic processes for NCs (McLaughlin et al. 2006). As such, this region is geometrically thin and the shell is effectively driven outwards by a transfer of momentum from the wind impacting on its inside.

The thrust on the shell from the CMO wind is proportional to the Eddington luminosity of the CMO (King & Pounds 2003; McLaughlin et al. 2006):

$$\frac{dp_{\text{wind}}}{dt} = \lambda \frac{L_{\text{Edd}}}{c} = \lambda \frac{4\pi GM_{\text{CMO}}}{\kappa}, \quad (3)$$

where  $M_{\text{CMO}}$  is the CMO mass and  $\kappa$  is the electron scattering opacity. For SMBHs,  $\lambda \sim 1$  (King & Pounds); for NCs,  $\lambda \sim 0.05$ , a value related to the mass fraction of the massive stars that contribute to the superwind (McLaughlin et al.).

As the shell moves outwards, the cooling time of the shocked wind material behind the shell eventually becomes longer than the dynamical time of the wind. This region then cannot cool before more material/energy is injected (King 2003; McLaughlin et al. 2006). As such, it expands and the shell becomes driven by the thermal pressure in the shocked wind region. If the shell can reach a galactocentric radius where this switch from momentum- to energy-driving occurs, then it may accelerate from that point to escape the galaxy (King 2003).

In this paper, we consider only the momentum-conserving phase of the feedback, in the form of a spherical supershell moving outwards into a spherical, dark-matter dominated protogalaxy, driven entirely by a steady wind from a central point mass that may be thought of as either an SMBH or an NC. Our aim is primarily to explore the effects of relaxing the assumption of isothermal dark matter distributions, so we leave to one side all issues around any transition to energy-driving, additional feedback from bulge-star formation, and evolution of the CMO mass.

The equation of motion that we consider for the shell is

$$\frac{d}{dt} [M_{\text{g}}(r)v] = \lambda \frac{L_{\text{Edd}}}{c} - \frac{GM_{\text{g}}(r)}{r^2} [M_{\text{CMO}} + M_{\text{DM}}(r)], \quad (4)$$

where  $r$  is the instantaneous radius of the shell;  $v = dr/dt$  is the velocity of the shell;  $M_{\text{DM}}(r)$  is the dark matter mass inside radius  $r$ ; and  $M_{\text{g}}(r)$  is the ambient gas mass originally inside radius  $r$  (i.e., the mass that has been swept up into

the shell when it has radius  $r$ ). The first term on the right-hand side of equation (4) is the wind thrust acting on the shell, from equation (3). The second and third terms on the right-hand side are the gravity of the CMO and the dark matter inside the shell (see also King 2005).

In general, we write  $M_{\text{g}}(r) = f_0 h(r) M_{\text{DM}}(r)$ , where  $f_0$  is a fiducial gas fraction ( $\approx 0.2$ ) and  $h(r)$  is a function that describes how the gas traces the dark matter; when  $h(r) \equiv 1$ , the gas directly traces the dark matter. It is also convenient to define characteristic mass and radius scales,  $M_{\sigma}$  and  $r_{\sigma}$ , in terms of a characteristic velocity dispersion  $\sigma_0$  in the dark matter halo:

$$\begin{aligned} M_{\sigma} &\equiv f_0 \kappa \sigma_0^4 / (\lambda \pi G^2) \simeq 4.56 \times 10^8 M_{\odot} \sigma_{200}^4 f_{0.2} \lambda^{-1} \\ r_{\sigma} &\equiv GM_{\sigma} / \sigma_0^2 \simeq 49.25 \text{ pc } \sigma_{200}^2 f_{0.2} \lambda^{-1}, \end{aligned} \quad (5)$$

where  $\sigma_{200} = \sigma_0/200 \text{ km s}^{-1}$  and  $f_{0.2} = f_0/0.2$ . Referring back to equation (1), the unit  $M_{\sigma}$  is just the critical CMO mass found by King (2005).

Then, defining  $\tilde{M} \equiv M/M_{\sigma}$ ,  $\tilde{r} \equiv r/r_{\sigma}$  and  $\tilde{v} \equiv v/\sigma_0$  equation (4) can be written

$$\begin{aligned} \frac{d}{d\tilde{r}} \left[ h^2 \tilde{M}_{\text{DM}}^2 \tilde{v}^2(\tilde{r}) \right] &= 8 \tilde{M}_{\text{CMO}} h(\tilde{r}) \tilde{M}_{\text{DM}}(\tilde{r}) \\ &- \frac{2h^2(\tilde{r}) \tilde{M}_{\text{DM}}^2(\tilde{r})}{\tilde{r}^2} \left[ \tilde{M}_{\text{CMO}} + \tilde{M}_{\text{DM}}(\tilde{r}) \right]. \end{aligned} \quad (6)$$

We aim to solve this equation for the velocity fields of momentum-driven shells,  $\tilde{v}^2(\tilde{r})$ , rather than  $\tilde{r}(t)$  explicitly.

If the wind thrust is great enough, then equation (6) will have solutions that allow shells to reach arbitrarily large  $\tilde{r}$  with non-zero  $\tilde{v}$ —the minimum requirement for escape of the feedback. If the wind thrust is unable to overcome the combined gravity of the CMO and dark matter then the shell will *stall* with  $\tilde{v}^2 = 0$  at some finite radius, and subsequently collapse. Equation (6) cannot describe such a collapse, since that would involve a shell with fixed mass rather than one that continually gathers mass [ $M_{\text{g}}(r) = f_0 h(r) M_{\text{DM}}(r)$ ] as it moves outwards into a galaxy.

The form of equation (6) allows us to select any density profile for the host galaxy dark matter and also allows for the segregation of gas and dark matter through the function  $h(r)$ . Throughout this paper, we consider only the case that  $h(r) \equiv 1$ , but we investigate various halo mass distributions.

## 3 THE SINGULAR ISOTHERMAL SPHERE

We look first at the dark matter density profile of a SIS, with  $h(\tilde{r}) \equiv 1$  so that gas traces the dark matter directly. Aspects of this case have been considered previously by several authors (Silk & Rees 1998; Fabian 1999; King 2003, 2005, 2010a; McLaughlin et al. 2006; Murray et al. 2005). King (2005, 2010a) looked at the behaviour of a shell that is far from an SMBH, so that the mass of dark matter inside the shell dominates over the SMBH gravity. King finds that the shell can reach arbitrarily large radii only if the black hole has the critical mass given in equation (1). However, as we now show, this condition does not actually guarantee that a momentum-driven shell will be able to make it to large enough radii that the CMO gravity becomes negligible compared to the dark matter.

The density of a SIS is given by

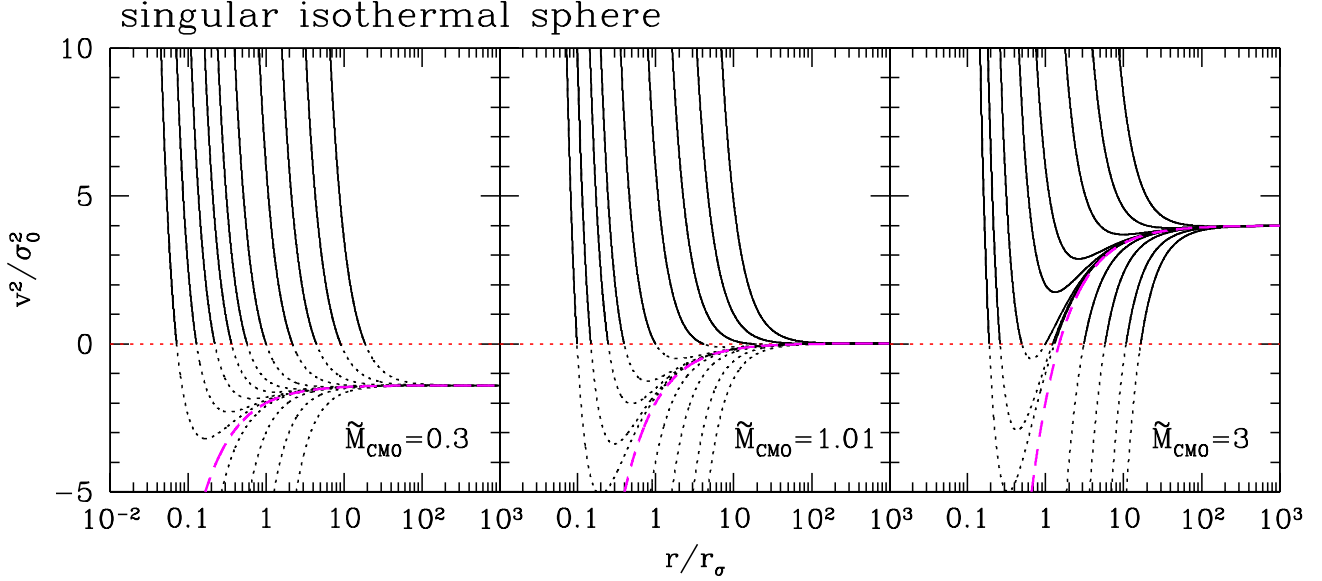


**Figure 1.** Velocity fields  $\tilde{v}^2$  versus  $\tilde{r}$  for momentum-driven shells in a SIS with spatially constant gas fraction and  $\tilde{M}_{\text{CMO}} = 0.3, 1.01$  and  $3$ . In each case, the solution with  $C = [\tilde{r} \tilde{v}(0)]^2 = 0$  is shown by a long-dashed (magenta) line. The physical ( $\tilde{v}^2 \geq 0$ ) parts of other solutions are shown as solid lines. All solutions with  $C < 0$  are unphysical at small radii, but if  $\tilde{M}_{\text{CMO}} > 1$  they will achieve  $\tilde{v}^2 \geq 0$  at large  $\tilde{r}$ , corresponding to launches. All solutions with  $C > 0$  decelerate from small radii. If one hits  $\tilde{v}^2 = 0$  at some point, then it generally becomes unphysical at larger radii, and the shell it describes must stall and collapse. This can occur even if  $\tilde{M}_{\text{CMO}} > 1$ . Formally, solutions with  $C > 0$  and  $\tilde{M}_{\text{CMO}} > 1$  that stall can have second physical parts with  $\tilde{v}^2 > 0$  at still larger  $\tilde{r}$ . These parts of such solutions again correspond to launches, though not of the same shells that stall at smaller radii.

$$\rho_{\text{DM}}(r) = \frac{\sigma_0^2}{2\pi G r^2}, \quad (7)$$

so that

$$M_{\text{DM}}(r) = 4\pi \int_0^r \rho_{\text{DM}}(r') r'^2 dr' = \frac{2\sigma_0^2}{G} r. \quad (8)$$

In terms of the characteristic mass and radius defined in equation (5), this means

$$\tilde{M}_{\text{DM}}(\tilde{r}) = 2\tilde{r}. \quad (9)$$

Then, with  $h(\tilde{r}) \equiv 1$ , equation (6) for the motion of the shell becomes

$$\frac{d}{d\tilde{r}} [\tilde{r}^2 \tilde{v}^2] = 4\tilde{M}_{\text{CMO}} \tilde{r} - 2\tilde{M}_{\text{CMO}} - 4\tilde{r}, \quad (10)$$

which has solution

$$\tilde{v}^2 = 2\tilde{M}_{\text{CMO}} - 2 - \frac{2\tilde{M}_{\text{CMO}}}{\tilde{r}} + \frac{C}{\tilde{r}^2}. \quad (11)$$

The constant of integration,  $C$ , represents (the square of) the shell's momentum,  $[M_{\text{g}}(r) v(r)]^2 \propto \tilde{r}^2 \tilde{v}^2$ , at  $\tilde{r} = 0$ .

In the limit of very large radius, equation (11) shows that the shell approaches a constant coasting speed:

$$\tilde{v}^2 \rightarrow 2\tilde{M}_{\text{CMO}} - 2. \quad (\tilde{r} \gg 1) \quad (12)$$

Equations (11) and (12) are implicit in King (2005) (multiply his eq. [2] by  $\dot{R}R$  and integrate). Equation (12) specifically is only physical if  $\tilde{v}^2 > 0$ . Thus, for the shell to have any chance of escaping we must have  $\tilde{M}_{\text{CMO}} > 1$ , which is exactly the result of King (2005, 2010a).

In the limit of small radius, the last term of equation (11) for  $\tilde{v}^2$  becomes dominant, and the initial momentum of the shell (i.e.,  $C$ ) determines the behaviour of the shell.

If  $C \leq 0$ , then  $\tilde{v}^2$  is large and negative at small radii, which is unphysical. However,  $d\tilde{v}^2/d\tilde{r} > 0$ , so it may happen that  $\tilde{v}^2 = 0$  at some larger radius and increases further outwards. The  $\tilde{v}^2 \geq 0$  part of such a solution is physical, and the point at which  $\tilde{v}^2 = 0$  can be considered as a ‘‘launch’’ radius for a (pre-existing) shell initially at rest.

A launch solution has  $\tilde{v}^2 = 0$  and  $d\tilde{v}^2/d\tilde{r} \geq 0$  at some  $\tilde{r}_{\text{launch}}$ . From equation (11), this requires

$$\tilde{r}_{\text{launch}}(\tilde{M}_{\text{CMO}} - 1) \geq \frac{\tilde{M}_{\text{CMO}}}{2}. \quad (13)$$

Thus, such solutions are only possible for  $\tilde{M}_{\text{CMO}} > 1$ , and then only starting from radii

$$\tilde{r}_{\text{launch}} \geq \frac{\tilde{M}_{\text{CMO}}}{2(\tilde{M}_{\text{CMO}} - 1)} > \frac{1}{2}. \quad (14)$$

As  $\tilde{M}_{\text{CMO}} \rightarrow 1$ ,  $\tilde{r}_{\text{launch}} \rightarrow \infty$ , so launches are not possible when  $\tilde{M}_{\text{CMO}} = 1$ .

If  $C > 0$ ,  $\tilde{v}^2$  is large and positive at small radii but  $d\tilde{v}^2/d\tilde{r} < 0$ , so the shell decelerates but keeps moving out into the galaxy, unless and until  $\tilde{v}^2 = 0$  is reached at some finite  $\tilde{r}$ . If this happens, then the shell stalls and is not able to escape. If  $\tilde{v}^2 = 0$  is never realised, then the shell is formally able to escape to large radii while purely momentum-driven.

The stall radius, at which  $\tilde{v}^2 = 0$ , is found from equation (11) as

$$\tilde{r}_{\text{stall}} = \frac{\tilde{M}_{\text{CMO}} - \sqrt{\tilde{M}_{\text{CMO}}^2 - 2C(\tilde{M}_{\text{CMO}} - 1)}}{2(\tilde{M}_{\text{CMO}} - 1)}, \quad (15)$$

where we have taken the root with the minus sign since this

corresponds to the first instance of  $\tilde{v}^2 = 0$  as the shell moves outwards. If  $\tilde{r}_{\text{stall}}$  is positive and finite, the shell cannot move out beyond this radius while purely momentum driven.

In the case that  $\tilde{M}_{\text{CMO}} < 1$ ,  $\tilde{r}_{\text{stall}} > 0$  for any  $C > 0$ . We can see this by noting that when  $\tilde{M}_{\text{CMO}} < 1$  the discriminant in equation (15) is always positive and  $> \tilde{M}_{\text{CMO}}^2$  so that both the numerator and denominator are negative, leading to a positive  $\tilde{r}_{\text{stall}}$ . As there are no physical launch solutions and the shell always stalls when  $\tilde{M}_{\text{CMO}} < 1$ , no shell can ever escape while purely momentum-driven if  $\tilde{M}_{\text{CMO}} < 1$ .

In the limit that  $\tilde{M}_{\text{CMO}} \rightarrow 1$ , we find that

$$\tilde{r}_{\text{stall}} = \frac{\tilde{M}_{\text{CMO}} - \tilde{M}_{\text{CMO}} \sqrt{1 - \frac{2C(\tilde{M}_{\text{CMO}} - 1)}{\tilde{M}_{\text{CMO}}^2}}}{2(\tilde{M}_{\text{CMO}} - 1)} \rightarrow \frac{C}{2}, \quad (16)$$

so  $\tilde{r}_{\text{stall}}$  occurs at some positive and finite radius when  $C > 0$  and, because  $\tilde{r}_{\text{launch}}$  is infinite (equation [14]), when  $\tilde{M}_{\text{CMO}} = 1$  exactly no shell can escape.

When  $\tilde{r}_{\text{stall}}$  does not exist (formally, when equation [15] is complex),  $\tilde{v}^2 = 0$  is never realised (for solutions with  $C > 0$ ) and the shell is able to reach arbitrarily large radii while being purely momentum-driven. This requires

$$\tilde{M}_{\text{CMO}}^2 - 2C(\tilde{M}_{\text{CMO}} - 1) < 0, \quad (17)$$

which, for  $\tilde{M}_{\text{CMO}} > 1$  (as we know this is the only case where purely momentum-driven escape is possible), means that escape requires

$$C > \frac{\tilde{M}_{\text{CMO}}^2}{2(\tilde{M}_{\text{CMO}} - 1)}. \quad (18)$$

If the value of  $C$  does not satisfy this constraint, then the shell will stall before ever reaching the radii where it could coast at the speed given by equation (12), even if  $\tilde{M}_{\text{CMO}} > 1$ . This is one reason why the critical CMO mass of King (2005, 2010a) is a *necessary but not sufficient* condition for the escape of momentum-driven CMO feedback from an isothermal sphere.

Figure 1 plots  $\tilde{v}^2$  versus  $\tilde{r}$  from equation (11) for  $\tilde{M}_{\text{CMO}} = 0.3, 1.01$  and  $3$ , with a range of  $C$  values in each case. The long-dashed (magenta) curve in each panel is the solution with  $C = 0$  for that  $\tilde{M}_{\text{CMO}}$ . The physical parts of solutions with  $C \neq 0$  are shown as solid lines

The left-hand panel of Figure 1 shows solutions for  $\tilde{M}_{\text{CMO}} = 0.3$ . No solution can escape in this case. Those with  $C > 0$  all stall at some finite radius (beyond which  $\tilde{v}^2 < 0$ ), while those with  $C \leq 0$  never give physical values of  $\tilde{v}^2 > 0$ .

Since we know that  $\tilde{M}_{\text{CMO}} = 1$  exactly also has no escape, the middle panel shows solutions for  $\tilde{M}_{\text{CMO}} = 1.01$ . In this case, only a few realistic solutions can “escape,” and those that do tend to a coasting speed of just  $v \sim 0.14\sigma_0$  at large radii (eq. [12]). In order even to reach the radii where this applies, shells must have very large velocity at small radii ( $C \gtrsim 51$  from equation [18], which corresponds to  $v \sim 0.2c$  at a distance of 1 pc from the CMO if  $\sigma_0 = 200 \text{ km s}^{-1}$ ), or else be launched somehow from very large radius ( $\tilde{r}_{\text{launch}} > 50.5$  from equation [14], which corresponds to  $r \gtrsim 2.5 \text{ kpc}$  if  $\sigma_0 = 200 \text{ km s}^{-1}$ ).

Finally, the right-hand panel of Figure 1 illustrates solutions for  $\tilde{M}_{\text{CMO}} = 3$ . Formally, all solutions now have a

significant coasting speed of  $2\sigma_0$  at large radii, but those with  $C < 9/4$  (or  $v \lesssim 15,000 \text{ km s}^{-1}$  at  $r = 1 \text{ pc}$  when  $\sigma_0 = 200 \text{ km s}^{-1}$ ) still stall before they are able to make it to large radius. Several of the solutions that escape are those with a launch radius; these require  $\tilde{r}_{\text{launch}} > 3/4$  ( $r \gtrsim 40 \text{ pc}$  for  $\sigma_0 = 200 \text{ km s}^{-1}$ ).

The escape speed from a truncated isothermal sphere is  $v_{\text{esc}} \gtrsim 2\sigma_0$  at large radius. Our results (equation [12] in particular) show that to achieve this escape speed requires  $\tilde{M}_{\text{CMO}} \gtrsim 3$ . This is another reason why the condition of King (2005, 2010a), i.e., simply  $\tilde{M}_{\text{CMO}} > 1$ , is necessary but not sufficient for the escape of a purely momentum-driven shell from an isothermal sphere. It is also, in essence, the same as the objection raised by Silk & Nusser (2010) against explanations of observed  $M_{\text{CMO}}$ - $\sigma$  relations as the result of outflows driven by the central objects alone. However, these and all other prior results have come from modelling protogalaxies only as SISs. We look now at the effect of allowing more realistic descriptions of dark-matter (and ambient gas) density profiles.

## 4 NON-ISOTHERMAL DARK MATTER HALOES

### 4.1 General analysis

Simulated dark matter haloes have density profiles that are shallower than that of an isothermal sphere at small radii and steeper than isothermal at large radii. Dubinski & Carlberg (1991) originally fitted haloes with the profile of Hernquist (1990), which has  $\rho_{\text{DM}} \propto r^{-1}$  at small radii and  $\rho_{\text{DM}} \propto r^{-4}$  at large radii. The dark-matter profile of Navarro, Frenk & White (1996, 1997) also has  $\rho_{\text{DM}} \propto r^{-1}$  at small radii, but  $\rho_{\text{DM}} \propto r^{-3}$  at large radii. Dehnen & McLaughlin (2005) develop a family of physically motivated halo models that, with  $\rho_{\text{DM}}(r)$  slightly shallower than  $r^{-1}$  at small radii and slightly steeper than  $r^{-3}$  at large radii, match current simulations at least as well as any other fitting function.

The circular speed corresponding to all such density profiles,  $V_c^2(r) = GM(r)/r$ , increases outwards from the centre, has a well-defined peak, and then declines towards larger radii. This suggests the peak of the circular speed curve as a natural point of reference for velocities, radii, and masses in realistically non-isothermal haloes.

We denote the location of the peak in  $V_c(r)$  by  $r_{\text{pk}}$  and the value  $V_c(r_{\text{pk}}) \equiv V_{c,\text{pk}}$ , and we define

$$\sigma_0^2 \equiv V_{c,\text{pk}}^2/2 \quad (19)$$

as a characteristic velocity dispersion in order to specify unique mass and radius units,  $\tilde{M}_\sigma$  and  $r_\sigma$ , as in equation (5) above. Then, recalling that  $\tilde{M} \equiv M/M_\sigma$ ,  $\tilde{r} \equiv r/r_\sigma$ , and  $\tilde{v} \equiv v/\sigma_0$ , so that  $\tilde{V}_c^2(\tilde{r}) = \tilde{M}_{\text{DM}}(\tilde{r})/\tilde{r}$ , we have

$$\tilde{V}_{c,\text{pk}}^2 = 2 \quad (20)$$

and

$$\tilde{M}_{\text{DM}}(\tilde{r}_{\text{pk}}) \equiv \tilde{M}_{\text{pk}} = 2\tilde{r}_{\text{pk}}. \quad (21)$$

We now refer all radii to the peak of the circular speed curve, defining  $x \equiv r/r_{\text{pk}}$ ; and we introduce a dimensionless mass profile,  $m(x)$ , such that

$$\tilde{M}_{\text{DM}}(x) \equiv \tilde{M}_{\text{pk}} m(x) . \quad (22)$$

By construction, then,

$$\tilde{M}_{\text{DM}}(1) \equiv \tilde{M}_{\text{pk}} \implies m(1) = 1 . \quad (23)$$

Moreover,  $\tilde{V}_c^2 = \tilde{M}_{\text{DM}}(\tilde{r})/\tilde{r} = 2m(x)/x$ , and thus,

$$\left( \frac{d\tilde{V}_c^2}{dx} \right)_{x=1} = 0 \implies \left( \frac{d \ln m}{d \ln x} \right)_{x=1} = 1 . \quad (24)$$

These generic properties of  $m(x)$  are important later in our analysis (see especially Appendix A).

With these definitions, equation (6) for the motion of a momentum-driven shell becomes

$$\frac{d}{dx} [h^2 m^2 \tilde{v}^2(x)] = 4\tilde{M}_{\text{CMO}} h(x)m(x) - 4 \frac{\tilde{M}_{\text{CMO}}}{\tilde{M}_{\text{pk}}} \frac{h^2(x)m^2(x)}{x^2} - 4 \frac{h^2(x)m^3(x)}{x^2} . \quad (25)$$

The formal solution of this, when  $h(x) \equiv 1$  for protogalactic gas that traces the dark matter directly, is

$$m^2(x) \tilde{v}^2(x) = C + 4\tilde{M}_{\text{CMO}} \int_0^x m(u) du - 4 \frac{\tilde{M}_{\text{CMO}}}{\tilde{M}_{\text{pk}}} \int_0^x \frac{m^2(u)}{u^2} du - 4 \int_0^x \frac{m^3(u)}{u^2} du , \quad (26)$$

where  $C \equiv m^2(0) \tilde{v}^2(0)$  is again a constant of integration representing (the square of) the momentum of the shell at the origin.

#### 4.1.1 Velocity fields at small and large radii

In the limit of small  $x$ , we can assume to leading order that

$$m(x) \longrightarrow A x^p , \quad (x \ll 1, p > 1) \quad (27)$$

where  $p > 1$  because we consider only halo density profiles that are shallower than isothermal at the centre. Equation (26) then gives

$$\tilde{v}^2 \longrightarrow \frac{C}{A^2} x^{-2p} , \quad (x \ll 1, C \neq 0) \quad (28)$$

so, as with the SIS, the integration constant, or (the square of) the momentum of the shell at  $r = 0$ , determines the behaviour of the shell.

If  $C > 0$ , then  $\tilde{v}^2 > 0$  and  $d\tilde{v}^2/dx < 0$  at small radii, and the shell decelerates outwards unless and until  $\tilde{v}^2 = 0$ , at which point the shell stalls and then collapses.

If  $C < 0$ , then  $\tilde{v}^2 < 0$  at small radii, which is unphysical; but  $d\tilde{v}^2/dx > 0$ , so  $\tilde{v}^2$  may become positive at some non-zero ‘‘launch’’ radius.

When  $C = 0$ , from equation (26),

$$\tilde{v}^2 \longrightarrow \frac{4\tilde{M}_{\text{CMO}}}{A} \frac{x^{1-p}}{p+1} - \frac{4\tilde{M}_{\text{CMO}}}{\tilde{M}_{\text{pk}}} \frac{x^{-1}}{2p-1} , \quad (x \ll 1, C = 0) \quad (29)$$

and the behaviour of the shell depends on the specific values of  $A$  and  $p$ , which in turn depend upon the specific choice of dark matter density profile. The solution with  $C = 0$  corresponds to a shell having zero momentum at  $x = 0$  and is also the value of  $C$  that separates initially decelerating

solutions that either escape or stall ( $C > 0$ ), from solutions that are launched from rest at a non-zero radius ( $C < 0$ ).

Since we consider only haloes that are steeper than isothermal at large radii, we must have that  $d \ln m/d \ln x < 1$  for  $x > 1$ . At large radius, the second term from the right-hand side of equation (26) then dominates, so that

$$\tilde{v}^2 \longrightarrow \frac{4\tilde{M}_{\text{CMO}}}{m^2(x)} \int_0^x m(u) du . \quad (x \gg 1) \quad (30)$$

The velocity field in the limit  $x \rightarrow \infty$  is therefore completely independent of initial conditions (i.e., no  $C$  dependence). To leading order,  $\tilde{v}^2 \rightarrow \mathcal{O}(x^{1-q})$  with  $q < 1$ . Thus, if the shell can make it to large radii at all in a non-isothermal halo it must eventually accelerate. This is in contrast to the SIS, where a shell at very large radius can only coast at a constant speed. It is the steeper-than-isothermal gradient of  $\rho_{\text{DM}}(r)$  at large radii in realistic dark matter haloes that leads to the acceleration.

#### 4.1.2 Condition for the escape of a particular shell

Any momentum-driven shell with a velocity field given by equation (26), and with  $C > 0$ , decelerates as it moves outwards from small radii according to equation (28). The same is true of shells with  $C = 0$ , if the small- $x$  value of  $\tilde{v}^2$  from equation (29) is positive. Some shells with  $C < 0$  and relatively small launch radii can also have  $\tilde{v}^2 > 0$  and  $d\tilde{v}^2/dx < 0$  over some range of radius (see below). Meanwhile, any solution to equation (25) [with  $h(x) \equiv 1$ ] accelerates at large radii according to equation (30). Therefore, there is a large class of solutions that go through local minima in  $\tilde{v}^2$  at intermediate radii. We want to know the CMO mass required for a particular shell in this class to escape a given galaxy. (The only solutions not in this class are some, with  $C < 0$ , which are launched from large enough radii that they only accelerate outwards, and so always escape.)

If a local minimum in  $\tilde{v}^2$  exists for a particular solution, we denote the radius where it occurs by  $x_{\text{min}}$ , and the value of the minimum by  $\tilde{v}_{\text{min}}^2$ . Putting  $h(x) \equiv 1$  in equation (25) and setting  $d\tilde{v}^2/dx = 0$  at  $x = x_{\text{min}}$ , we then obtain

$$\tilde{v}_{\text{min}}^2 \frac{d \ln m^2(x_{\text{min}})}{d \ln x_{\text{min}}} = 4\tilde{M}_{\text{CMO}} \frac{x_{\text{min}}}{m(x_{\text{min}})} - 4 \frac{\tilde{M}_{\text{CMO}}}{\tilde{M}_{\text{pk}}} \frac{1}{x_{\text{min}}} - 4 \frac{m(x_{\text{min}})}{x_{\text{min}}} . \quad (31)$$

If a shell with a given initial momentum (value of  $C$ ) is to escape a dark-matter halo with given  $m(x)$ ,  $\tilde{M}_{\text{pk}}$ , and  $\sigma_0 \equiv V_{c,\text{pk}}/\sqrt{2}$ , then we must have  $\tilde{v}_{\text{min}}^2 \geq 0$  so the shell does not stall (i.e., cross  $\tilde{v}^2 = 0$ ) before it can start accelerating outwards. We refer to the case that  $\tilde{v}_{\text{min}}^2 = 0$  exactly as the *critical* case, and we denote the values of  $\tilde{M}_{\text{CMO}}$  and  $x_{\text{min}}$  in this case by  $\tilde{M}_{\text{crit}}$  and  $x_{\text{crit}}$ . Then, from equation (31),

$$\tilde{M}_{\text{crit}} = \frac{m^2(x_{\text{crit}})}{x_{\text{crit}}^2} \left[ 1 - \frac{1}{\tilde{M}_{\text{pk}}} \frac{m(x_{\text{crit}})}{x_{\text{crit}}^2} \right]^{-1} . \quad (32)$$

Also, setting  $x = x_{\text{crit}}$ ,  $\tilde{v}^2 = 0$ , and  $\tilde{M}_{\text{CMO}} = \tilde{M}_{\text{crit}}$  in equation (26), and using equation (32) to eliminate  $\tilde{M}_{\text{pk}}$ , yields

$$\tilde{M}_{\text{crit}} = \frac{\int_0^{x_{\text{crit}}} [m(x_{\text{crit}}) - m(u)] [m(u)/u]^2 du + C/4}{\int_0^{x_{\text{crit}}} [x_{\text{crit}}^2/m(x_{\text{crit}}) - u^2/m(u)] [m(u)/u]^2 du} .$$

(33)

Equating the right-hand sides of equation (32) and (33) allows us to solve for  $x_{\text{crit}}$ , and then  $\tilde{M}_{\text{crit}}$ , in terms of  $C$  and the dark-matter halo parameters. The *necessary* condition for the escape of a purely momentum-driven shell with a particular value of  $C$  is just  $\tilde{M}_{\text{CMO}} \geq \tilde{M}_{\text{crit}}$ .

Equation (32) can give a sensible (positive) value for  $\tilde{M}_{\text{crit}}$  only for shell-and-dark matter combinations such that  $\tilde{M}_{\text{pk}} > m(x_{\text{crit}})/x_{\text{crit}}^2$ . This is not a problem in general.  $\tilde{M}_{\text{pk}}$  is the dark matter mass inside the peak of the dark-matter circular-speed curve, in units of  $M_\sigma \simeq 4.6 \times 10^8 M_\odot \sigma_{200}^4$  (equation [5]), and so will be a large number in real galaxies. Meanwhile, the function  $m(x)/x^2$  is always equal to 1 at  $x = 1$  (equation [23]), so that having  $\tilde{M}_{\text{pk}} > m(x_{\text{crit}})/x_{\text{crit}}^2$  at some reasonable value of  $x_{\text{crit}}$  is usually assured.

The density profiles of realistic dark-matter halo models are such that  $d \ln m / d \ln x < 2$  in the main, the only exception being in the very innermost regions of some models (see below). Thus, for most values of  $x_{\text{crit}}$ , the integral in the denominator of equation (33) is positive; while the integral in the numerator is always positive. Therefore, this equation implies  $\tilde{M}_{\text{crit}} > 0$  for any shell with  $C \geq 0$ . Launch solutions with *modest*  $C < 0$  can also have  $\tilde{M}_{\text{crit}} > 0$ , so long as the numerator in equation (33) is still positive. If  $C$  is too large and negative, then formally  $\tilde{M}_{\text{crit}} < 0$ , which means that such solutions do not actually go through minima in  $\tilde{v}^2$ . These correspond to shells, launched from large radii, which accelerate monotonically outwards to escape regardless of the CMO mass.

Below, we will find the necessary  $\tilde{M}_{\text{crit}}$  for shells that have  $C = 0$  (i.e., zero momentum at zero radius) in some specific dark-matter haloes. We emphasize, however, that this is not the only physically meaningful solution. Solutions with  $C > 0$  would describe shells that receive an impulse at the centre. Solutions with  $C < 0$  could be of interest for shells that stall at some radius inside a galaxy during an early phase of CMO growth, and are later “re-launched” by feedback from the CMO when it is more massive.

#### 4.1.3 Sufficient condition for the escape of any shell

Momentum-driven shells with different initial conditions ( $C$  values) have different values of  $x_{\text{crit}}$  and  $\tilde{M}_{\text{crit}}$ , given by equations (32) and (33). To compare these values between different shell solutions, we differentiate equation (32) with respect to  $x_{\text{crit}}$ , for a fixed dark matter mass  $\tilde{M}_{\text{pk}}$ :

$$\frac{d\tilde{M}_{\text{crit}}}{dx_{\text{crit}}} = \frac{2m^2(x_{\text{crit}})x_{\text{crit}}}{\left[x_{\text{crit}}^2 - m(x_{\text{crit}})/\tilde{M}_{\text{pk}}\right]^2} \times \left\{ \left[ \frac{d \ln m(x_{\text{crit}})}{d \ln x_{\text{crit}}} - 1 \right] - \frac{1}{2\tilde{M}_{\text{pk}}} \frac{1}{x_{\text{crit}}} \frac{dm(x_{\text{crit}})}{dx_{\text{crit}}} \right\}. \quad (34)$$

By definition,  $(d \ln m / d \ln x - 1) = d \ln V_c^2 / d \ln x$ , which is positive at  $x < 1$  and negative for  $x > 1$  (recall equation [24]). Hence,  $d\tilde{M}_{\text{crit}}/dx_{\text{crit}} > 0$  among shells with sufficiently small  $x_{\text{crit}}$ , and  $d\tilde{M}_{\text{crit}}/dx_{\text{crit}} < 0$  among shells with sufficiently large  $x_{\text{crit}}$ . Setting  $d\tilde{M}_{\text{crit}}/dx_{\text{crit}} = 0$  for a given dark-matter  $m(x)$  and  $\tilde{M}_{\text{pk}}$  therefore identifies the momentum-

driven shell that has the *largest* critical CMO mass required for escape,  $\tilde{M}_{\text{crit}}^{\text{max}}$ .

To find  $\tilde{M}_{\text{crit}}^{\text{max}}$ , we first solve the equation  $d\tilde{M}_{\text{crit}}/dx_{\text{crit}} = 0$  for the radius  $x_{c,\text{max}}$  at which the shell with exactly this critical mass begins to accelerate,

$$\left. \frac{d \ln m}{d \ln x} \right|_{x=x_{c,\text{max}}} = 1 + \frac{1}{2\tilde{M}_{\text{pk}}} \frac{1}{x_{c,\text{max}}} \left. \frac{dm}{dx} \right|_{x=x_{c,\text{max}}}, \quad (35)$$

and then use this value in equation (32):

$$\tilde{M}_{\text{crit}}^{\text{max}} = \frac{m^2(x_{c,\text{max}})}{x_{c,\text{max}}^2} \left[ 1 - \frac{1}{\tilde{M}_{\text{pk}}} \frac{m(x_{c,\text{max}})}{x_{c,\text{max}}^2} \right]^{-1}. \quad (36)$$

The *sufficient* condition for the escape of *any* momentum-driven shell is simply  $\tilde{M}_{\text{CMO}} \geq \tilde{M}_{\text{crit}}^{\text{max}}$ . This trivially includes any launch solutions of the type, mentioned above, that do not go through local minima in  $\tilde{v}^2$  but only ever accelerate outwards.

We analyze equations (35) and (36) further in Appendix A. There we show that, in the observationally relevant limit of large halo mass  $\tilde{M}_{\text{pk}}$ ,

$$\begin{aligned} x_{c,\text{max}} &\rightarrow 1 + \frac{1}{2\tilde{M}_{\text{pk}}} \left( \left. \frac{d^2 m}{dx^2} \right|_{x=1} \right)^{-1} \\ \tilde{M}_{\text{crit}}^{\text{max}} &\rightarrow 1 + \frac{1}{\tilde{M}_{\text{pk}}} \quad (\tilde{M}_{\text{pk}} \gg 1) \end{aligned} \quad (37)$$

to first order in  $(1/\tilde{M}_{\text{pk}})$ . That is, in very massive, non-isothermal dark matter haloes, the CMO mass that suffices to ensure the escape of any momentum-driven shell tends to the value  $\tilde{M}_{\text{crit}}^{\text{max}} \rightarrow 1$ ; and the radius where the slowest-moving shell driven by a CMO with this mass begins to accelerate tends to  $x_{c,\text{max}} \rightarrow 1$ , which is the peak of the dark-matter circular-speed curve.

#### 4.1.4 $M$ - $\sigma$ and $M$ - $V_c$ relations

The dimensional CMO mass that guarantees the escape of any momentum-driven shell from a non-isothermal halo follows from recalling the definition of the mass unit  $M_\sigma$  (equation [5]) and our identification of a characteristic velocity dispersion in terms of peak circular speed in the halo (equation [19]). For very massive haloes in particular ( $M_{\text{pk}} \gg M_\sigma$ ), equation (37) gives approximately

$$M_{\text{crit}}^{\text{max}} \rightarrow M_\sigma \equiv \frac{f_0 \kappa}{\lambda \pi G^2} \sigma_0^4 \equiv \frac{f_0 \kappa}{\lambda \pi G^2} \frac{V_{c,\text{pk}}^4}{4}. \quad (38)$$

Numerically,

$$M_{\text{crit}}^{\text{max}} \rightarrow 1.14 \times 10^8 M_\odot \left( \frac{V_{c,\text{pk}}}{200 \text{ km s}^{-1}} \right)^4 f_{0.2} \lambda^{-1}, \quad (39)$$

in which  $\lambda \sim 1$  describes CMOs that are supermassive black holes, while  $\lambda \sim 0.05$  applies for nuclear star clusters (King & Pounds 2003; McLaughlin et al. 2006).

This result reduces to the  $M$ - $\sigma$  relation obtained by King (2005) for SISs, in which  $V_c = \sqrt{2} \sigma_0$  is constant with radius. However, there are significant distinctions between previous work and our new analysis.

First, as we have emphasized,  $M_{\text{crit}}^{\text{max}}$  corresponds in the isothermal case to a CMO mass that is *necessary but not sufficient* for momentum-driven feedback to break out of a galaxy; while in the non-isothermal case it is a *sufficient but*

not always necessary CMO mass. The CMO masses required for the escape of most momentum-driven shells in a given dark-matter halo (as obtained from equations [32] and [33] above) will be smaller than  $M_{\text{crit}}^{\text{max}}$ . On these grounds alone, theoretical  $M_{\text{crit}}^{\text{max}}-\sigma_0$  or  $M_{\text{crit}}^{\text{max}}-V_{c,\text{pk}}$  relations from our work are expected to be something of upper limits to observed  $M-\sigma$  or  $M-V_c$  relations.

Second, our general treatment shows that the value of  $M_{\text{crit}}^{\text{max}}$  in equation (38) or (39) applies only *in the limit of very large dark-matter halo mass*,  $M_{\text{pk}} \gg M_\sigma$ . The exact value of the sufficient CMO mass  $M_{\text{crit}}^{\text{max}}$  for a specific value of  $M_{\text{pk}}$  must be obtained from equations (35) and (36).

Third, our results are the first to incorporate explicitly and rigorously the peak value of a dark-matter circular-speed curve (and associated velocity dispersion), which is a well-defined quantity in *any* realistic non-isothermal halo. This provides a new basis from which to begin addressing observational claims of correlations between CMO masses and dark-matter halo properties (e.g., Volonteri et al. 2011; Ferrarese 2002).

In the rest of this section, we illustrate the general results we have obtained, by looking in detail at their application to three specific dark-matter halo models.

#### 4.2 Hernquist model haloes

The first non-isothermal density profile we consider is that of Hernquist (1990). This model has been used to fit dark-matter haloes from N-body simulations (e.g., Dubinski & Carlberg 1991) and also has the advantage that, with it, our problem remains analytically tractable.

The density of a Hernquist sphere is given by

$$\rho_{\text{DM}}(r) = \frac{M_{\text{tot}}}{2\pi r_0^3} \left(\frac{r}{r_0}\right)^{-1} \left(1 + \frac{r}{r_0}\right)^{-3}, \quad (40)$$

where  $r_0$  is a scale radius and  $M_{\text{tot}}$  is the total halo mass. In terms of the characteristic mass and radius of equation (5), the mass enclosed inside radius  $\tilde{r}$  is

$$\tilde{M}_{\text{DM}}(\tilde{r}) = \tilde{M}_{\text{tot}} \left(\frac{\tilde{r}/\tilde{r}_0}{1 + \tilde{r}/\tilde{r}_0}\right)^2. \quad (41)$$

The circular-speed curve for this model,  $\tilde{V}_c^2 = \tilde{M}_{\text{DM}}(\tilde{r})/\tilde{r}$ , peaks at  $\tilde{r}_{\text{pk}} = \tilde{r}_0$ , so that the mass inside this radius is

$$\tilde{M}_{\text{DM}}(\tilde{r}_{\text{pk}}) \equiv \tilde{M}_{\text{pk}} = \frac{\tilde{M}_{\text{tot}}}{4}. \quad (42)$$

Defining  $x \equiv r/r_{\text{pk}} = r/r_0$ , we therefore write

$$\tilde{M}_{\text{DM}}(x) = \tilde{M}_{\text{pk}} \frac{4x^2}{(1+x)^2} \equiv \tilde{M}_{\text{pk}} m(x). \quad (43)$$

With the above definitions and  $h(x) \equiv 1$  again, equation (25) for the motion of a momentum-driven shell has the general solution

$$\tilde{v}^2 = \tilde{M}_{\text{CMO}} \left(\frac{1+x}{x}\right)^4 \left[1 + x - \frac{1}{1+x} - 2\ln(1+x)\right] - \frac{4}{3} \frac{\tilde{M}_{\text{CMO}}}{\tilde{M}_{\text{pk}}} \frac{1+x}{x} - \frac{16}{5} \frac{x}{1+x} + \frac{C}{16} \left(\frac{1+x}{x}\right)^4. \quad (44)$$

In the limit that  $x \rightarrow 0$ ,  $m(x) \rightarrow 4x^2$ , and from equation (28) we have

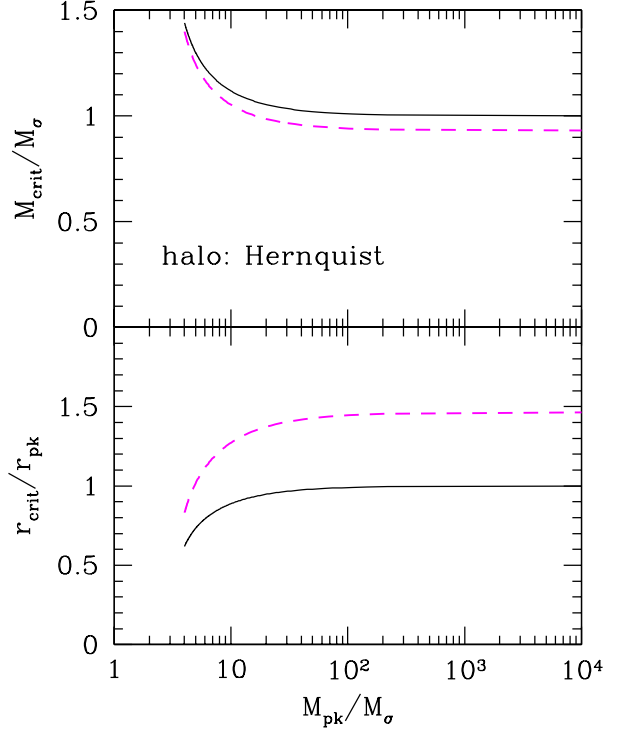


**Figure 2.** Solid lines show, as functions of  $\tilde{M}_{\text{pk}}$ , the sufficient critical CMO mass,  $\tilde{M}_{\text{crit}}^{\text{max}}$ , that allows the escape of any momentum-driven shell from a Hernquist halo (upper panel); and the radius,  $x_{c,\text{max}}$ , at which the slowest-moving shell driven by such a CMO begins to accelerate to escape (lower panel). Dashed lines show the necessary  $\tilde{M}_{\text{crit}}$  and associated  $x_{\text{crit}}$  for the escape of the particular  $\tilde{M}_{\text{pk}}$  solution with  $C = 0$ . We show results only for halo masses  $\tilde{M}_{\text{pk}} \geq 4$ , above which  $x_{\text{crit}}$  and  $x_{c,\text{max}}$  are single-valued functions of  $\tilde{M}_{\text{pk}}$ .

$$\tilde{v}^2 \rightarrow \frac{C}{16} x^{-4}, \quad (x \ll 1, C \neq 0) \quad (45)$$

or, if  $C = 0$ , equation (29) instead gives

$$\tilde{v}^2 \rightarrow \left[ \frac{\tilde{M}_{\text{CMO}}}{3} - \frac{4}{3} \frac{\tilde{M}_{\text{CMO}}}{\tilde{M}_{\text{pk}}} \right] x^{-1}. \quad (x \ll 1, C = 0) \quad (46)$$

Thus, for halo masses  $\tilde{M}_{\text{pk}} > 4$ , all shell solutions with  $C \geq 0$  decelerate from large, positive  $\tilde{v}^2$  at small radii.

In the large- $x$  limit,  $m(x) \rightarrow 4$  and equation (30) gives

$$\tilde{v}^2 \rightarrow \tilde{M}_{\text{CMO}} x. \quad (x \gg 1) \quad (47)$$

All solutions tend to the same form at large radii, corresponding to acceleration outwards that is independent of  $C$ , as we expect from the general discussion in §4.1

The solid lines in Figure 2 show, as functions of  $\tilde{M}_{\text{pk}}$ , the sufficient CMO mass,  $\tilde{M}_{\text{crit}}^{\text{max}}$ , that provides for the escape of *any* momentum-driven shell from a Hernquist halo (upper panel); and the radius,  $x_{c,\text{max}}$  at which the slowest-moving shell begins to accelerate towards larger radii (lower panel). These quantities have been calculated from equations (35) and (36), with  $m(x)$  defined in equation (43). As expected on general grounds (see equation [37]; also Appendix A),  $\tilde{M}_{\text{crit}}^{\text{max}} \rightarrow 1$  and  $x_{c,\text{max}} \rightarrow 1$  (denoting the peak of the circular-speed curve in the halo) for large  $\tilde{M}_{\text{pk}} \gg 1$ .

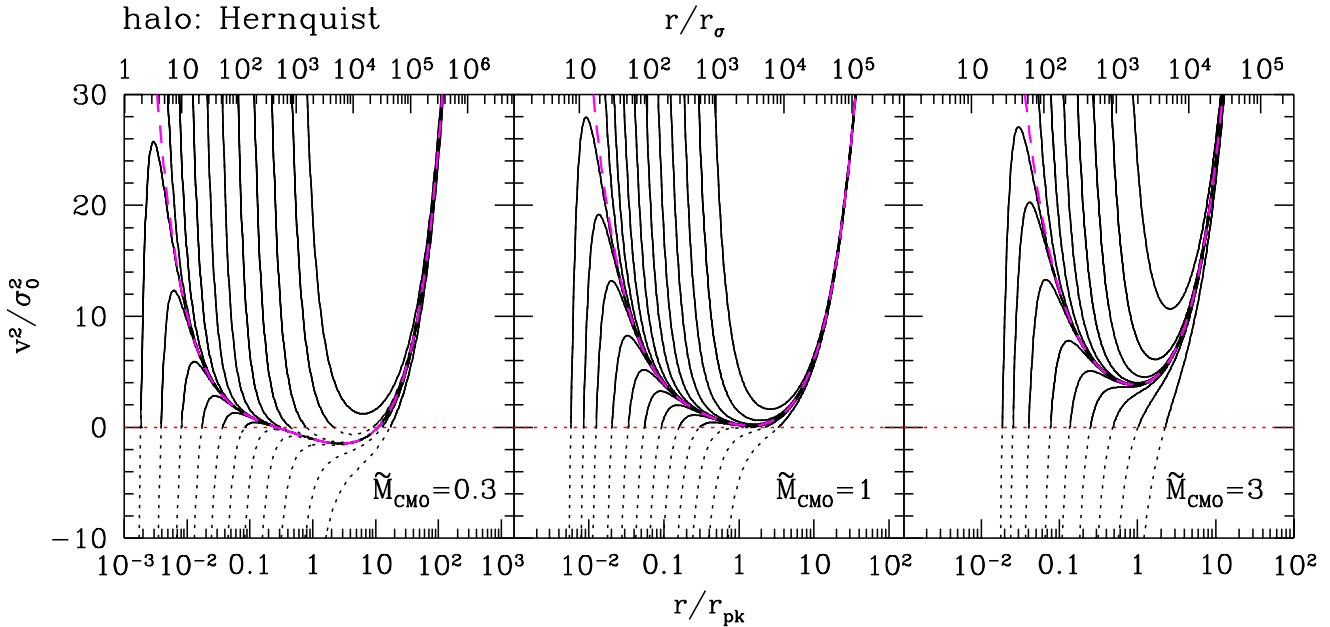


**Figure 3.** Velocity fields  $\tilde{v}^2(x)$  for  $\tilde{M}_{\text{CMO}} = 0.3, 1, 3$  in a Hernquist dark-matter halo with spatially constant gas fraction and dimensionless  $\tilde{M}_{\text{pk}} = 4000$ . This corresponds to a roughly Milky Way-sized halo with  $r_{\text{pk}} \approx 50$  kpc,  $M_{\text{pk}} \approx 4.7 \times 10^{11} M_{\odot}$ , and  $\sigma_0 \approx 140$  km s $^{-1}$ . The top axis gives the radius in units of  $r_{\sigma} \approx 25$  pc  $\sigma_{140}^2 f_{0.2} \lambda^{-1}$ , where  $f_{0.2} = f_0/0.2$ . The magenta curve represents the solution with  $C = 0$  for each value of CMO mass illustrated. As in Figure 1, the physical part(s) of each solution are shown by the solid lines.

The dashed lines in Figure 2 show the necessary CMO mass,  $\tilde{M}_{\text{crit}}$ , that allows for the escape from a Hernquist halo of shells with  $C = 0$  [ $m^2 \tilde{v}^2 \rightarrow 0$  as  $x \rightarrow 0$ ] specifically; and the radius,  $x_{\text{crit}}$ , at which this particular shell begins to accelerate outwards. In this case,  $\tilde{M}_{\text{crit}}$  and  $x_{\text{crit}}$  have been calculated from equations (32) and (33), with  $C$  set to zero and  $m(x)$  taken from equation (43). Now, the necessary  $\tilde{M}_{\text{crit}} \rightarrow 0.93$  in the limit  $\tilde{M}_{\text{pk}} \rightarrow \infty$  (versus the *sufficient*  $\tilde{M}_{\text{crit}}^{\text{max}} \rightarrow 1$ ), and the acceleration begins at  $x_{\text{crit}} \rightarrow 1.46$  (just beyond the corresponding radius for  $\tilde{M}_{\text{CMO}} = \tilde{M}_{\text{crit}}^{\text{max}}$ ).

Parameters that give a reasonable, model-independent summary of the circular-speed curve of the Milky Way dark-matter halo are  $r_{\text{pk}} \approx 50$  kpc and  $V_{\text{c,pk}} \approx 200$  km s $^{-1}$  (see, e.g., Dehnen et al. 2006; McMillan 2011). Thus,  $M_{\text{pk}} = r_{\text{pk}} V_{\text{c,pk}}^2 / G \approx 4.7 \times 10^{11} M_{\odot}$ ;  $\sigma_0 \equiv V_{\text{c,pk}} / \sqrt{2} \approx 140$  km s $^{-1}$ ; and  $M_{\sigma} \approx 1.1 \times 10^8 M_{\odot} f_{0.2} \lambda^{-1}$ , so that  $\tilde{M}_{\text{pk}} \approx 4300$ .

Figure 3 shows the solutions from equation (44) for  $\tilde{M}_{\text{CMO}} = 0.3, 1$  and  $3$  in a Hernquist halo with  $\tilde{M}_{\text{pk}} = 4000$ . In each panel the dashed (magenta) curve shows the solution with  $C = 0$ . As in Figure 1, the physical parts of each solution (i.e., those with  $\tilde{v}^2 \geq 0$ ) are shown as solid lines.

The left panel shows solutions with  $\tilde{M}_{\text{CMO}} = 0.3$ . Most of these represent shells that stall and cannot escape. Unlike the SIS however, it is possible to have launch solutions when  $\tilde{M}_{\text{CMO}} < 1$ . Solutions with  $C < 0$  but very close to zero are launched from inside  $\tilde{r}_{\text{pk}}$  and initially accelerate, then reach a maximum velocity and decelerate. When  $\tilde{M}_{\text{CMO}} = 0.3$ , these solutions all stall at a finite radius. Solutions launched from outside  $\tilde{r}_{\text{pk}}$  either correspond to large and negative  $C$  or are the formal continuations of solutions that stall at smaller radii, go into the unphysical  $\tilde{v}^2 < 0$  regime, but then later recover to  $\tilde{v}^2 > 0$ . All launch solutions of this type accelerate

monotonically towards larger radii and therefore escape; but, for this value of  $\tilde{M}_{\text{CMO}}$ , they all start from infeasibly large launch radii of order  $x \sim 10$  (i.e.,  $r \sim 10 r_{\text{pk}} \sim 500$  kpc) or more. For large enough *positive* values of  $C$  it is possible for a shell to escape without stalling (or being launched from a large radius) when  $\tilde{M}_{\text{CMO}} = 0.3$ , although this is again a formal result that is not physically plausible. The uppermost curve in the left panel of Figure 3 shows one solution that evidently only requires  $\tilde{M}_{\text{crit}} < 0.3$  to escape this halo; but it has  $C \gtrsim 10$ , which, given that  $r_{\text{pk}} \approx 50$  kpc and  $\sigma_0 \approx 140$  km s $^{-1}$ , corresponds to a shell velocity of  $\sim 10^6 c$  at a radius of 1 pc.

The middle panel of Figure 3 shows solutions for  $\tilde{M}_{\text{CMO}} = 1$ . All of the solutions shown are able to escape the halo. However, from equation (37), we know that, with  $\tilde{M}_{\text{pk}} = 4000$ , the CMO mass sufficient to ensure escape is actually  $\tilde{M}_{\text{CMO}}^{\text{max}} \approx 1.00025$ . Thus, there are some shells in a (narrow) range of  $C$  values very close to 0 that stall rather than escape; these are simply not shown here. Several solutions are shown that have  $C < 0$  but close to 0. These are launched from inside the peak of the circular-speed curve and, though they come very close to stalling, those shown manage eventually to accelerate and escape to large radii. Several launch solutions with large and negative  $C$  are also shown, all starting from radii  $r > r_{\text{pk}}$  and all accelerating to escape. The solution with  $C = 0$  exactly is seen to escape (as do all solutions above it with  $C > 0$ ), which is expected since our calculations above (see Figure 2) gave  $\tilde{M}_{\text{crit}} \simeq 0.93$  for this solution.

The right-hand panel of Figure 3 shows velocity-field solutions for  $\tilde{M}_{\text{CMO}} = 3$ . This is well above the value of the sufficient  $\tilde{M}_{\text{crit}}^{\text{max}}$  given by equations (35) and (36) above (or, approximately, equation [37]). As a result, and in contrast to

the SIS, all shells are able to escape and there are no stalls, regardless of the initial shell momentum.

### 4.3 NFW model haloes

We next consider the dark matter density profile of Navarro, Frenk & White (1996, 1997; NFW), which has

$$\rho_{\text{DM}}(r) = 4\rho_s \left(\frac{r}{r_s}\right)^{-1} \left(1 + \frac{r}{r_s}\right)^{-2}, \quad (48)$$

where  $r_s$  is a scale radius and  $\rho_s$  is the density at  $r_s$ . From this,

$$M_{\text{DM}}(r) = 16\pi r_s^3 \rho_s \left[ \ln(1 + r/r_s) - \frac{r/r_s}{1 + r/r_s} \right], \quad (49)$$

and it follows that the circular-speed curve,  $V_c^2 = GM_{\text{DM}}(r)/r$ , peaks at  $\mathcal{R} \equiv r_{\text{pk}}/r_s \simeq 2.16258$ . Thus, with  $x \equiv r/r_{\text{pk}}$  we have

$$\tilde{M}_{\text{DM}}(x=1) \equiv \tilde{M}_{\text{pk}} = 16\pi r_s^3 \rho_s \left[ \ln(1 + \mathcal{R}) - \frac{\mathcal{R}}{1 + \mathcal{R}} \right], \quad (50)$$

and

$$\tilde{M}_{\text{DM}}(x) = \tilde{M}_{\text{pk}} \frac{\ln(1 + \mathcal{R}x) - \mathcal{R}x/(1 + \mathcal{R}x)}{\ln(1 + \mathcal{R}) - \mathcal{R}/(1 + \mathcal{R})} \equiv \tilde{M}_{\text{pk}} m(x). \quad (51)$$

At small radii, then, the dimensionless mass profile tends to

$$m(x) \rightarrow \frac{\mathcal{R}^2 x^2}{2} \left[ \ln(1 + \mathcal{R}) - \frac{\mathcal{R}}{1 + \mathcal{R}} \right]^{-1}, \quad (x \ll 1) \quad (52)$$

implying for the velocity field, from equation (28) for  $C \neq 0$ ,

$$\tilde{v}^2 \rightarrow \frac{4C}{\mathcal{R}^4} \left[ \ln(1 + \mathcal{R}) - \frac{\mathcal{R}}{1 + \mathcal{R}} \right]^2 x^{-4}, \quad (x \ll 1, C \neq 0) \quad (53)$$

or from equation (29) for  $C = 0$ ,

$$\tilde{v}^2 \rightarrow \left( \frac{8}{3} \left[ \ln(1 + \mathcal{R}) - \frac{\mathcal{R}}{1 + \mathcal{R}} \right] \frac{\tilde{M}_{\text{CMO}}}{\mathcal{R}^4} - \frac{4}{3} \frac{\tilde{M}_{\text{CMO}}}{\tilde{M}_{\text{pk}}} \right) x^{-1}. \quad (x \ll 1, C = 0) \quad (54)$$

For  $\tilde{M}_{\text{pk}} \gtrsim 5.001$ ,  $\tilde{v}^2$  tends to a positive value in the limit of small  $x$  for  $C = 0$ , and then all shells with  $C \geq 0$  decelerate from large, positive velocities at small radii.

In the limit that  $x \rightarrow \infty$ , the NFW mass profile diverges logarithmically,

$$m(x) \rightarrow \left[ \ln(1 + \mathcal{R}) - \frac{\mathcal{R}}{(1 + \mathcal{R})} \right]^{-1} \ln(\mathcal{R}x) \quad (x \gg 1) \quad (55)$$

and, from equation (30), all shell velocities tend to

$$\tilde{v}^2 \rightarrow \frac{4\tilde{M}_{\text{CMO}}}{[\ln(\mathcal{R}x)]^2} \left[ \ln(1 + \mathcal{R}) - \frac{\mathcal{R}}{1 + \mathcal{R}} \right] [x \ln(\mathcal{R}x) - x]. \quad (x \gg 1) \quad (56)$$

The solid lines in Figure 4 show, as functions of  $\tilde{M}_{\text{pk}}$ , the sufficient CMO mass that allows for the escape of *any* momentum-driven shell from an NFW halo (upper panel); and the radius,  $x_{c,\text{max}}$ , at which the slowest-moving shell

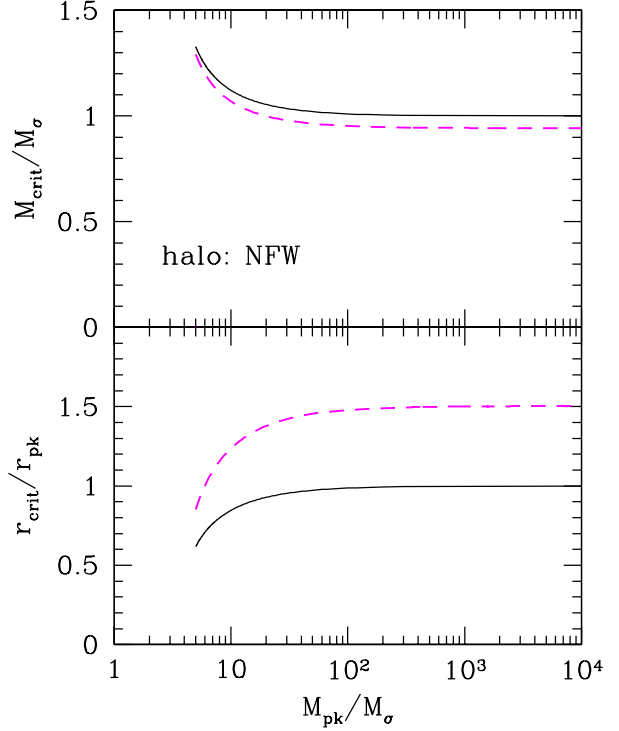


**Figure 4.** Solid lines show, as functions of  $\tilde{M}_{\text{pk}}$ , the CMO mass  $\tilde{M}_{\text{crit}}^{\text{max}}$ , which is sufficient for the escape of any momentum-driven shell from an NFW halo (upper panel); and the radius  $x_{c,\text{max}}$ , at which the slowest-moving shell begins to accelerate to escape (lower panel). Dashed lines show the necessary values of  $\tilde{M}_{\text{crit}}$ , and the associated radii  $x_{\text{crit}}$ , for the escape of the particular solution with  $C = 0$ . Results are shown for  $\tilde{M}_{\text{pk}} \gtrsim 5$ , above which  $x_{\text{crit}}$  and  $x_{c,\text{max}}$  are single-valued functions of  $\tilde{M}_{\text{pk}}$ .

begins to accelerate (lower panel). These are again calculated from equations (35) and (36), now with  $m(x)$  given by equation (51). In the limit of large  $\tilde{M}_{\text{pk}}$ ,  $\tilde{M}_{\text{crit}}^{\text{max}} \rightarrow 1$  and  $x_{c,\text{max}} \rightarrow 1$  again, just as found for the Hernquist halo in Figure 2 and as expected in general from equation (37) and Appendix A.

The dashed lines in Figure 4 show the critical CMO mass that is necessary for the escape from NFW haloes of shells with  $C = 0$  specifically; and the radii,  $x_{\text{crit}}$  at which these particular shells begin to accelerate for a given  $\tilde{M}_{\text{pk}}$ . In this case,  $\tilde{M}_{\text{crit}}$  and  $x_{\text{crit}}$  are calculated from equations (32) and (33). In the limit of large  $\tilde{M}_{\text{pk}}$ , we have  $\tilde{M}_{\text{crit}} \rightarrow 0.94$ , again slightly smaller than the CMO mass sufficient to ensure the escape of any shell. The acceleration begins at  $x_{\text{crit}} \rightarrow 1.50$ , again somewhat larger than  $x_{c,\text{max}}$  in the sufficient case.

Given  $m(x)$  in equation (51), equation (26) for the velocity fields of momentum-driven shells in NFW haloes must be evaluated numerically. Figure 5 shows several of the solutions for dimensionless CMO masses  $\tilde{M}_{\text{CMO}} = 0.3, 1$  and  $3$ , and with  $\tilde{M}_{\text{pk}} = 4000$  for a Milky Way-sized halo (see §4.2). In each panel of this figure, the dashed (magenta) line shows the solution with  $C = 0$ . As in Figures 1 and 3, the physical parts of solutions with  $C \neq 0$  are shown by solid lines.

Figure 5 is qualitatively similar to Figure 3 for shells in Hernquist (1990) haloes. The left-hand panel, which plots

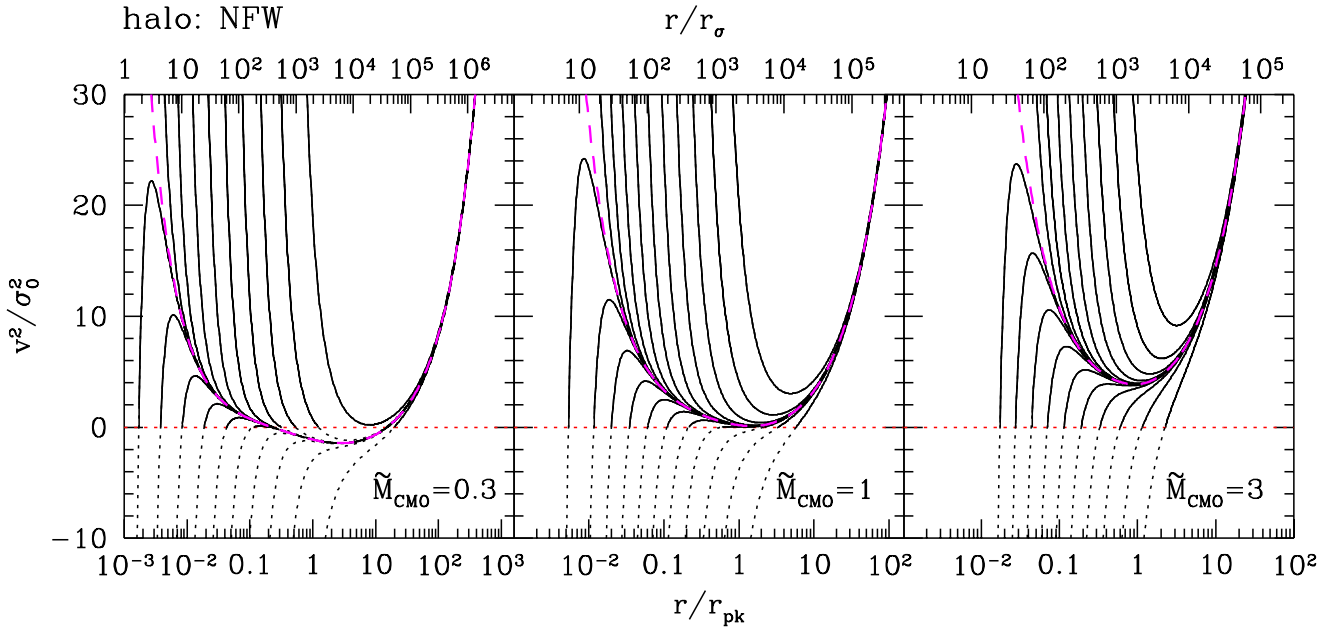


**Figure 5.** Velocity fields  $\tilde{v}^2(x)$  for  $\tilde{M}_{\text{CMO}} = 0.3, 1$  and  $3$  in an NFW halo with spatially constant gas fraction and  $\tilde{M}_{\text{pk}} = 4000$ . Radius is shown in units of  $r_\sigma \approx 25 \text{ pc } \sigma_{140}^2 f_{0.2} \lambda^{-1}$  along the top axis, and in units of  $r_{\text{pk}} \approx 50 \text{ kpc}$  along the bottom axis. The dashed, magenta curve in each panel represents the solution with  $C = 0$  for that value of  $\tilde{M}_{\text{CMO}}$ . The physical part(s) of all other solutions are shown as solid lines.

solutions for a modest  $\tilde{M}_{\text{CMO}} = 0.3$ , shows all physically plausible shells with  $C \geq 0$  stalling and unable to escape the halo. (The one such solution shown that is able to escape, given this CMO mass, has  $C \gtrsim 20$ , corresponding to  $v \sim 10^6 c$  at  $r = 1 \text{ pc}$ .) Solutions with  $C < 0$  include those that are launched from within  $r < r_{\text{pk}}$ , which first accelerate but then decelerate and stall; and those launched from outside  $r > r_{\text{pk}}$ , which accelerate monotonically outwards and always escape, but which all start from large  $r \gtrsim 500 \text{ kpc}$ .

The middle panel shows solutions for  $\tilde{M}_{\text{CMO}} = 1$ . All of those shown escape, including those with  $C < 0$  but near zero, which are launched from  $r < r_{\text{pk}}$ . There are solutions within a narrow range of  $C$  values near zero that cannot escape. These are not shown, but they exist because, given that  $\tilde{M}_{\text{pk}} = 4000$  here, the critical CMO mass required for the escape of all possible solutions is  $\tilde{M}_{\text{crit}}^{\text{max}} \approx 1.00025 > 1$ , according to equation (37). The solution with  $C = 0$  is able to escape, as the CMO mass necessary to expel it from such a massive halo is  $\tilde{M}_{\text{crit}} \simeq 0.94 < 1$  (see Figure 4).

The right-hand panel of Figure 5 confirms again that all shells escape easily when  $\tilde{M}_{\text{CMO}} > \tilde{M}_{\text{crit}}^{\text{max}}$ .

#### 4.4 Dehnen & McLaughlin model haloes

Finally, we consider a dark-matter density profile from the family developed by Dehnen & McLaughlin (2005). Their models are analytical solutions to the spherical Jeans equation, which have “pseudo” phase-space density profiles,  $\rho(r)/\sigma^3(r)$ , that are power laws in radius and closely match those found in cosmological  $N$ -body simulations. They also allow for radially varying anisotropy in the dark-matter velocity dispersion; and they fit the spherically averaged den-

sity profiles of simulated haloes as well as, or better than, any other fitting function proposed to date.

The halo model of Dehnen & McLaughlin that is isotropic at its centre has the density distribution

$$\rho_{\text{DM}}(r) = \frac{5}{9} \frac{M_{\text{tot}}}{\pi r_0^3} \left(\frac{r}{r_0}\right)^{-7/9} \left[1 + \left(\frac{r}{r_0}\right)^{4/9}\right]^{-6}, \quad (57)$$

where  $r_0$  is a scale radius and  $M_{\text{tot}}$  is the total halo mass. This gives the enclosed mass profile,

$$M_{\text{DM}}(r) = M_{\text{tot}} \left[ \frac{(r/r_0)^{4/9}}{1 + (r/r_0)^{4/9}} \right]^5. \quad (58)$$

The circular-speed curve in this case peaks at  $r_{\text{pk}}/r_0 = (11/9)^{9/4}$ , so now we set  $x \equiv \tilde{r}/\tilde{r}_{\text{pk}} = (9/11)^{9/4} (r/r_0)$ . Then,

$$\tilde{M}_{\text{DM}}(x=1) \equiv \tilde{M}_{\text{pk}} = \left(\frac{11}{20}\right)^5 \tilde{M}_{\text{tot}} \quad (59)$$

and

$$\tilde{M}_{\text{DM}}(x) = \tilde{M}_{\text{pk}} \left(\frac{20}{11}\right)^5 \left(\frac{\frac{11}{9}x^{4/9}}{1 + \frac{11}{9}x^{4/9}}\right)^5 \equiv \tilde{M}_{\text{pk}} m(x). \quad (60)$$

When  $x$  is small,  $m(x) \rightarrow (20/9)^5 x^{20/9}$ , and from equation (28) the momentum-driven shell velocity field for  $C \neq 0$  tends to

$$\tilde{v}^2 \rightarrow C \left(\frac{9}{20}\right)^{10} x^{-40/9}; \quad (x \ll 1, C \neq 0) \quad (61)$$

or, from equation (29) if  $C = 0$ ,

$$\tilde{v}^2 \rightarrow \frac{36}{29} \left(\frac{9}{20}\right)^5 \tilde{M}_{\text{CMO}} x^{-11/9}. \quad (x \ll 1, C = 0) \quad (62)$$

When  $x$  is large,  $m(x) \rightarrow (20/11)^5$  and equation (30) gives

$$\tilde{v}^2 \rightarrow 4 \left(\frac{11}{20}\right)^5 \tilde{M}_{\text{CMO}} x. \quad (x \gg 1) \quad (63)$$

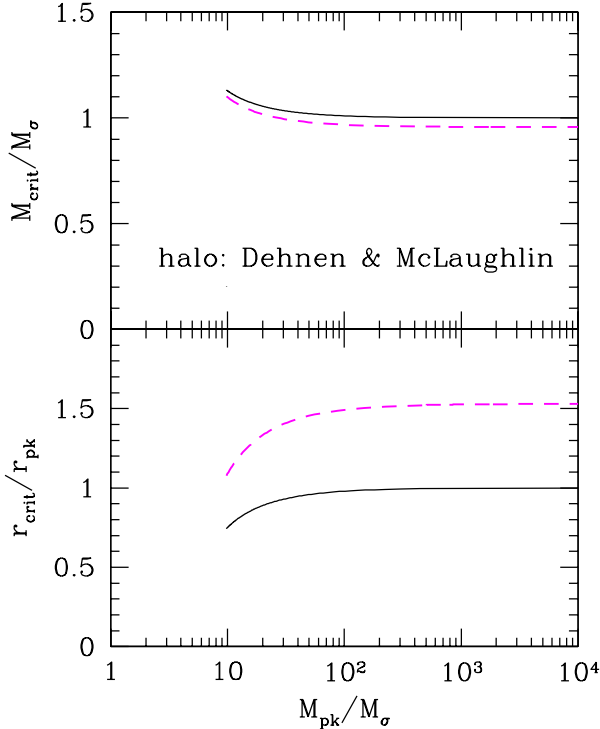


**Figure 6.** Solid lines show, as functions of  $\tilde{M}_{\text{pk}}$ , the CMO mass,  $\tilde{M}_{\text{crit}}^{\text{max}}$ , that is sufficient to ensure the escape of any momentum-driven shell from a Dehnen & McLaughlin (2005) halo (upper panel); and the radius,  $x_{\text{c,max}}$ , at which the slowest-moving shell begins to accelerate to escape (lower panel). Dashed lines show the necessary  $\tilde{M}_{\text{crit}}$ , and the associated  $x_{\text{crit}}$ , for the escape of shells with  $C = 0$  specifically. Results are shown for  $\tilde{M}_{\text{pk}} \gtrsim 10$ , since then  $x_{\text{crit}}$  and  $x_{\text{c,max}}$  are single-valued functions of  $\tilde{M}_{\text{pk}}$ .

The solid lines in Figure 6 show, as functions of  $\tilde{M}_{\text{pk}}$ , the CMO mass  $\tilde{M}_{\text{crit}}^{\text{max}}$ , which is sufficient for the escape of any momentum-driven shell from this halo (upper panel); and the radius  $x_{\text{c,max}}$  at which the slowest-moving shell driven by a CMO with the sufficient mass begins to accelerate outwards (lower panel). These are calculated as usual from equations (35) and (36), with  $m(x)$  in equation (60). As for the other haloes we have looked at, and as will always be true in general,  $\tilde{M}_{\text{crit}}^{\text{max}} \rightarrow 1$  and  $x_{\text{c,max}} \rightarrow 1$  for  $\tilde{M}_{\text{pk}} \gg 1$ .

The dashed lines in Figure 6 show the necessary CMO mass  $\tilde{M}_{\text{crit}}$ , and the radius  $x_{\text{crit}}$  at which acceleration begins, for the escape of shells with  $C = 0$ , calculated from equations (32) and (33). In the limit of large  $\tilde{M}_{\text{pk}}$ ,  $\tilde{M}_{\text{crit}} \rightarrow 0.96$  in this case, and  $x_{\text{crit}} \rightarrow 1.53$ .

With  $m(x)$  in equation (60), the solutions to equation (25) with  $h(x) \equiv 1$  must again be obtained numerically. Figure 7 shows solutions for several shells in a Dehnen & McLaughlin (2005) halo with  $\tilde{M}_{\text{pk}} = 4000$  (again as in §4.2), for each of the CMO masses  $\tilde{M}_{\text{CMO}} = 0.3, 1$  and  $3$ . The solution with  $C = 0$  in each case is shown by a dashed (magenta) line, and the physical part(s) of  $C \neq 0$  solutions are drawn as solid lines.

Figure 7 is similar in all respects to Figures 3 and 5 for the other non-isothermal halo models we have examined. The left-hand panel of the figure shows again that

with  $\tilde{M}_{\text{CMO}} < 1$ , all physically interesting solutions correspond to shells that stall. Launch solutions with  $C < 0$  that escape must start from impractically large  $r \gtrsim 500$  kpc. Solutions with  $C > 0$  require  $C \gtrsim 30$  to escape, which implies unphysical shell speeds at small radii (i.e.,  $v \gtrsim 10^6 c$  at 1 pc). The middle panel of Figure 7 confirms that  $\tilde{M}_{\text{CMO}} = 1$  is *almost* sufficient for the escape of all momentum-driven shells; there are a few solutions with a narrow range of  $C$  values near  $C = 0$  that cannot escape (because in fact  $\tilde{M}_{\text{crit}}^{\text{max}} \approx 1 + 1/\tilde{M}_{\text{pk}} = 1.00025$  here), but which are not shown. The right-hand panel finally illustrates again how any shell, with any initial conditions, can escape the halo when  $\tilde{M}_{\text{CMO}}$  exceeds the sufficient  $\tilde{M}_{\text{crit}}^{\text{max}}$  given by equations (35) and (36) in general.

## 5 SUMMARY AND DISCUSSION

We have analyzed the motion of momentum-conserving supershells driven into isothermal and non-isothermal protogalaxies by steady (time-independent) winds from central massive objects (CMOs: either supermassive black holes or nuclear star clusters). Our main goal has been to find the critical CMO mass that can drive a supershell to escape a galaxy, essentially clearing it of ambient gas and stopping further CMO growth. Having such a critical CMO mass as a function of a characteristic dark-matter halo velocity dispersion then gives a theoretical  $M_{\text{CMO}}-\sigma$  relation.

We assumed that the CMO wind thrust is proportional to  $M_{\text{CMO}}$  (through the Eddington luminosity: King & Pounds 2003; McLaughlin et al. 2006) to obtain a general equation of motion for momentum-driven shells (equation [6] or [25]) that allows for any dark-matter halo mass profile and also for the segregation of gas and dark matter. We solved this equation for  $v^2(r)$ , the (square of the) shell velocity as a function of radius in the CMO’s host galaxy, for a number of different dark-matter density profiles, though only ever considering the case that gas traces dark matter directly. This analysis extends and generalizes others in the literature, which have only considered dark-matter haloes described as SISs, and which have not presented full solutions for the velocity fields of momentum-driven supershells.

Since our main aim was to clarify the effect on theoretical  $M-\sigma$  relations of relaxing the simplifying assumption that CMOs are embedded in singular isothermal dark matter haloes, we retained some other simplifications also adopted by previous authors. One of these is the assumption that the wind driving the CMO feedback is time-independent—in essence, that the CMO mass is constant throughout the motion of a momentum-conserving supershell. In reality, of course, if the CMO is a black hole emitting at the Eddington limit, then it is also accreting mass at the Eddington rate; thus, a wind thrust proportional to  $M_{\text{CMO}}$  must grow on the Salpeter timescale of  $\sim 4-5 \times 10^7$  yr. If the CMO is a nuclear star cluster, then the duration and strength of a superwind from it is tied to the star-formation history and to the main-sequence lifetime of supernova progenitors.

The other simplification we made was to consider only the momentum-driven phase of supershell evolution, ignoring any eventual transition to the energy-driven regime. Further work is needed to incorporate gas cooling properly into a fuller treatment of *time-dependent* feedback, which will

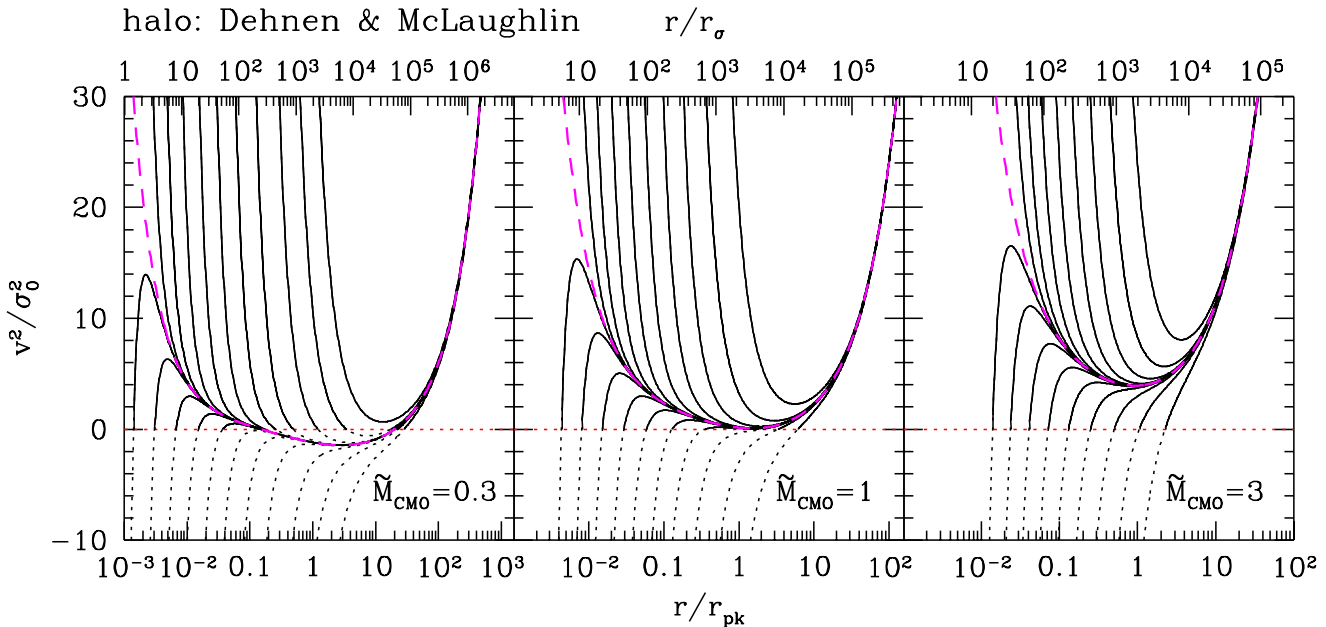


**Figure 7.** Velocity fields  $\tilde{v}^2(x)$  for CMO masses  $\tilde{M}_{\text{CMO}} = 0.3, 1$  and  $3$  in a Dehnen & McLaughlin (2005) dark-matter halo with spatially constant gas fraction and  $\tilde{M}_{\text{pk}} = 4000$ . Radius is in units of  $r_\sigma \approx 25 \text{ pc } \sigma_{140}^2 f_{0.2} \lambda^{-1}$  along the top axis, and in units of  $r_{\text{pk}} \approx 50 \text{ kpc}$  (for a Milky Way-sized halo) along the bottom axis. The solution with  $C = 0$  is shown by a dashed (magenta) line in each panel. As in Figures 1, 3, and 5, the physical part(s) of all other solutions are shown as solid lines.

also account for the impact of variable CMO masses and wind strengths on  $M$ - $\sigma$  relations.

### 5.1 The singular isothermal sphere

Revisiting the case of a galaxy modelled as a SIS, we showed in §3 that at large radii a momentum-driven shell tends to a constant coasting speed given by equation (12):

$$v^2 \longrightarrow v_\infty^2 \equiv 2\sigma_0^2 \left[ \frac{M_{\text{CMO}}}{M_\sigma} - 1 \right], \quad (r \rightarrow \infty, \text{ SIS}) \quad (64)$$

in which (cf. King 2005)

$$M_\sigma \equiv \frac{f_0 \kappa}{\lambda \pi G^2} \sigma_0^4 \simeq 4.56 \times 10^8 M_\odot \sigma_{200}^4 f_{0.2} \lambda^{-1}, \quad (65)$$

where  $\sigma_0$  is the velocity dispersion of the halo and  $\sigma_{200} \equiv \sigma_0 / (200 \text{ km s}^{-1})$ ;  $f_0 \approx 0.2$  is a fiducial gas mass fraction; and the parameter  $\lambda \simeq 1$  if the CMO is a supermassive black hole (SMBH), or  $\lambda \approx 0.05$  if the CMO is a nuclear star cluster (NC; McLaughlin et al. 2006). This shows that a momentum-conserving shell can reach arbitrarily large radii in an isothermal sphere, and potentially escape, only if the CMO driving the shell has a mass  $M_{\text{CMO}} > M_\sigma$  (so that  $v_\infty^2 > 0$ ). Otherwise, any shell must stall at some finite radius, and subsequently collapse, until the CMO grows in mass and drives a stronger wind (see also King 2005).

The critical  $M_{\text{CMO}}$  value in equation (65) has previously been obtained by methods that did not include solving explicitly for  $v^2(r)$  (see King 2003, 2005, 2010a; Murray et al. 2005; McLaughlin et al. 2006). By solving for the full velocity fields  $v^2(r)$  of momentum-driven shells, we have shown that, while  $M_{\text{CMO}} \geq M_\sigma$  is *necessary*, it is *not sufficient* to guarantee the escape of momentum-driven CMO winds from isothermal spheres.

First, as discussed in §3,  $M_{\text{CMO}}$  and the initial momentum of a shell very near a CMO *together* determine whether the shell can reach large enough radii to achieve the asymptotic coasting speed,  $v_\infty$ ; if it cannot, then the value of  $v_\infty$ , which is determined by  $M_{\text{CMO}}$  alone, is immaterial. As an example, when  $M_{\text{CMO}} = 1.01 M_\sigma$ , a shell will stall at a finite radius, and re-collapse, unless its launch from the CMO gives it an exceedingly fast velocity of  $v \gtrsim 0.2 c \sigma_{200}$  at a radius of  $r \simeq 1 \text{ pc } \sigma_{200}^2$ .

Second, if a shell is to coast at large radii with the nominal “escape” velocity from an isothermal sphere—that is, with  $v_\infty > 2\sigma_0$ —then our work shows that  $M_{\text{CMO}} > 3M_\sigma$  is required. This would mean CMO masses almost an order of magnitude higher, at a given  $\sigma_0$ , than those provided by the observed  $M$ - $\sigma$  relations for either SMBHs or NCs. This is, in essence, the objection raised by Silk & Nusser (2010) to the idea that momentum-driven CMO winds are the sole source of  $M$ - $\sigma$ . However, the objection—and detailed answers to it, whether involving additional feedback from bulge-star formation triggered by the CMO outflow (Silk & Nusser 2010) or a transition to energy-conserving evolution at some large shell radius (Power et al. 2011; King et al. 2011)—applies *only* if the host galaxy of a CMO is an isothermal sphere.

### 5.2 Non-isothermal haloes

More realistic descriptions of dark-matter haloes have density profiles that are shallower at small radii than the  $r^{-2}$  profile of an isothermal sphere, and steeper than  $r^{-2}$  at large radii. Therefore, they have circular-speed curves,  $V_c^2(r) = GM(r)/r$ , with well-defined peaks. We showed that, in *any* such non-isothermal halo, any momentum-driven shell must begin to accelerate beyond some large radius and will even-

tually exceed the halo escape velocity, just so long as the CMO wind driving the shell can push it to the radius where it starts accelerating. We obtained equations that can be solved for the critical CMO mass,  $M_{\text{crit}}$ , required for the escape of a shell with a given initial momentum in any halo with a peaked  $V_c(r)$  curve (§4.1.2; equations [32] and [33]). We then showed that there is a largest critical CMO mass,  $M_{\text{crit}}^{\text{max}}$ , in any such halo. Once a CMO exceeds this mass, *any* momentum-driven shell can escape the halo (§4.1.3). Our equations (35) and (36) allow the calculation of  $M_{\text{crit}}^{\text{max}}$  in general and provide a *sufficient* condition for the escape of momentum-driven feedback from non-isothermal haloes.

In this general analysis, a basic mass unit  $M_\sigma$  is defined in terms of the peak circular speed in a halo:

$$\begin{aligned} M_\sigma &\equiv \frac{f_0 \kappa}{\lambda \pi G^2} \frac{V_{\text{c,pk}}^4}{4} \\ &= 1.14 \times 10^8 M_\odot f_{0.2} \lambda^{-1} \left( \frac{V_{\text{c,pk}}}{200 \text{ km s}^{-1}} \right)^4. \end{aligned} \quad (66)$$

In the most relevant case that haloes are much more massive than  $M_\sigma$ , the sufficient condition for the escape of momentum-driven feedback is (equation [37])

$$M_{\text{CMO}} \geq M_{\text{crit}}^{\text{max}} = M_\sigma \left[ 1 + \frac{M_\sigma}{M_{\text{pk}}} + \mathcal{O} \left( \frac{M_\sigma^2}{M_{\text{pk}}^2} \right) \right], \quad (M_{\text{pk}} \gg M_\sigma) \quad (67)$$

where  $M_{\text{pk}} = r_{\text{pk}} V_{\text{c,pk}}^2 / G$  is the mass of dark matter inside the radius where the halo circular speed peaks. For the Milky Way,  $M_{\text{pk}} \approx 4000 M_\sigma$ , so this condition is  $M_{\text{CMO}} \gtrsim M_\sigma$  to a good approximation in intermediate and massive galaxies.

In a SIS,  $V_c = \sqrt{2} \sigma_0$  is constant and, in effect,  $M_{\text{pk}} = \infty$ , so formally  $M_{\text{crit}}^{\text{max}}$  and  $M_\sigma$  reduce to equation (65). Although important differences remain between the isothermal and non-isothermal cases, this suggests that the most appropriate single velocity dispersion to use to characterize an entire non-isothermal halo, at least in discussions of  $M$ – $\sigma$  relations, is simply  $\sigma_0 \equiv V_{\text{c,pk}} / \sqrt{2}$ .

We illustrated the application of our general results by solving for the velocity fields of momentum-driven shells in three specific models of non-isothermal dark-matter haloes (Hernquist 1990—§4.2; Navarro et al. 1996, 1997—§4.3; Dehnen & McLaughlin 2005—§4.4). We noted that there are two main types of  $v^2(r)$  solutions, corresponding to shells that decelerate from small radii close to the CMO (going on to accelerate further out if  $M_{\text{CMO}}$  is large enough, or to stall at a finite radius if not), and shells that are launched from zero velocity at non-zero radii (and may then either stall or escape at larger radii). We also saw that the radius at which any particular shell starts to accelerate to escape a halo is typically within a factor of order unity times the radius at which the dark-matter circular speed peaks (which is some tens of kpc in a Milky Way-sized halo).

Since  $M_{\text{CMO}} \geq M_{\text{crit}}^{\text{max}} \approx M_\sigma$  is a *sufficient* condition for the escape of momentum-driven feedback from non-isothermal haloes, it generally *exceeds* the minimally *necessary* condition for the escape of any one particular shell. In the specific haloes that we looked at, shells with zero initial momentum reach large radii and accelerate to escape for any  $M_{\text{CMO}} \gtrsim (0.93\text{--}0.96) M_\sigma$ . Different initial conditions may enable escape for still (slightly) lower CMO masses.

The fact that  $M_{\text{CMO}} \geq M_{\text{crit}}^{\text{max}}$  allows all purely

momentum-conserving shells in non-isothermal haloes to *accelerate* at large radii—rather than just to coast as in isothermal spheres, at potentially sub-escape speeds even if  $M_{\text{CMO}} > M_\sigma$ —effectively answers the main objection of Silk & Nusser (2010) to momentum-driven feedback from CMO winds as the direct cause of observed  $M$ – $\sigma$  relations.

**Again, these results are for time-independent winds from CMOs with fixed masses. We have integrated  $v(r)$  to find  $r(t)$  for the  $C = 0$  momentum-driven shells in each of the non-isothermal haloes calculated in §§4.2–4.4. For  $M_{\text{CMO}} = M_{\text{crit}}^{\text{max}}$ , these shells take  $\sim 3\text{--}4 \times 10^8$  yrs to move from  $r = 0$  to  $r \sim r_{\text{pk}}$ , from where they can accelerate to escape the galaxy. In the case that the CMO is an SMBH, this corresponds to  $\sim 7\text{--}8$  Salpeter times. Thus, if a critical mass black hole were to launch a momentum-driven shell from  $r = 0$ , the hole would be a factor of  $\sim e^{7\text{--}8}$  times more massive by the time the shell escapes. Our expression for the sufficient  $M_{\text{crit}}^{\text{max}}$  as a function of  $V_{\text{c,pk}}$  (eq. [67]) would then presumably estimate a *lower limit* to observed SMBH  $M$ – $\sigma$  relations. However, this apparent difficulty will be mitigated by two effects.**

First, if SMBHs grew from much smaller seeds, then even in the case of purely momentum-driven feedback the supershells of swept-up ambient gas will have already been driven to large radii by the time the black hole reaches the critical mass. The question then becomes, for a given mass-accretion history, how near to  $r = r_{\text{pk}}$  is a supershell at the time that the black hole attains our critical mass; and can the shell subsequently move out to  $r_{\text{pk}}$ , and start to accelerate, within less than another Salpeter time? To answer this will require solving a fully time-dependent problem including CMO masses and wind thrusts that (in the SMBH case at least) increase monotonically with time. Whatever the final result, it is clear that any upwards “correction” to our  $M_{\text{crit}}$  for steady winds and momentum-conserving shells will be substantially *less* than a factor of  $\sim e^{7\text{--}8}$ .

Second, the time required for a shell to reach a radius at which it can accelerate to escape a galaxy will be *less* than any time we derive, whether for steady or time-dependent winds, if the shell transitions from momentum-conserving to energy-conserving at some radius (say,  $r_{\text{trans}}$ ), inside  $r_{\text{pk}}$ . This will happen if the cooling time of the shocked gas in the shell exceeds the dynamical time of the wind at  $r = r_{\text{trans}}$  (cf. King 2003; McLaughlin et al. 2006). The issue then becomes to find the CMO mass at the time when  $r = r_{\text{trans}}$ , rather than the mass when  $r = r_{\text{pk}}$ .

These considerations emphasize the need to include both cooling processes and time-dependent winds in future, more sophisticated analyses of CMO feedback-regulated galaxy formation. Meanwhile, it is worth noting how tantalizingly close the  $M$ – $\sigma$  relations contained in our present work already are to the observed scalings.

### 5.3 Observational implications

**Although subject to the indicated caveats about time-dependent winds and pure momentum-driving,** our results directly predict a relation between SMBH (or NC) masses and the dark-matter haloes of their host galaxies, through the peak circular speed of the haloes (equa-

tions [66] and [67], for the large- $M_{\text{pk}}$  limit specifically). This provides a basis for understanding relations between SMBH mass and dark-matter halo mass or asymptotic circular speed, which have been claimed (e.g., Ferrarese 2002; Volonteri et al. 2011), though also contested (Ho 2007; Kormendy & Bender 2011), on empirical grounds. It is important to recognize the physical content of such a CMO–dark matter relation, in a feedback context. It does *not* suggest that dark matter in any way feeds the growth of either black holes or nuclear star clusters (cf. Kormendy et al. 2011). Rather, it reflects the fact that the gravity of a host galaxy, which is dominated by its dark matter halo, is what ultimately determines whether the feedback from a CMO can escape. The more familiar  $M$ - $\sigma$  relation has the same fundamental interpretation in this picture.

Making explicit the connection between a theoretical halo  $V_{\text{c,pk}}$  and an observed stellar  $\sigma$ , or even an asymptotic circular speed in real galaxies (which will include contributions from baryons as well as dark matter), is a nontrivial task and beyond the scope of our current discussion. We simply recall here that the observed relation between SMBH mass and the stellar velocity dispersion averaged over one effective radius in a sample of early-type galaxies and bulges analyzed by Gültekin et al. (2009) is

$$M_{\text{bh}} \simeq (1.32 \pm 0.24) \times 10^8 M_{\odot} \left( \frac{\sigma_{\text{eff}}}{200 \text{ km s}^{-1}} \right)^{4.24 \pm 0.41}; \quad (68)$$

while the relation inferred by Volonteri et al. (2011) between SMBH mass and the *asymptotic* circular speed in a subset of the same systems is

$$M_{\text{bh}} \simeq (2.45 \pm 0.80) \times 10^7 M_{\odot} \left( \frac{V_{\text{c,a}}}{200 \text{ km s}^{-1}} \right)^{4.22 \pm 0.93}. \quad (69)$$

If we were to associate our  $V_{\text{c,pk}}$  and  $\sigma_0 \equiv V_{\text{c,pk}}/\sqrt{2}$  in non-isothermal haloes directly with observational estimates of  $V_{\text{c,a}}$  and  $\sigma_{\text{eff}}$ , then we might conclude that the normalizations of the predicted  $M_{\text{CMO}}-V_{\text{c,pk}}$  and  $M_{\text{CMO}}-\sigma$  relations exceed the observed normalizations by factors of  $\approx 3$ –4. This point has previously been made, from comparisons only with an isothermal-sphere analysis, by King (2010b).

**However, before too much is made of any normalization offset, or even the caveats associated with steady winds and pure momentum-driving**, it is crucial that the correct relationships be worked out in detail (within specific dark-matter halo models, and accounting properly for the segregation of dark matter and stars) between  $V_{\text{c,pk}}$  and  $V_{\text{c,a}}$ , and between  $\sigma_0 \equiv V_{\text{c,pk}}/\sqrt{2}$  and the stellar  $\sigma_{\text{eff}}$ . It is probably also relevant that we (like other authors) have worked with the assumption that the gas in protogalaxies directly traces the dark matter. The consequences of relaxing this assumption remain unclear, although our general equation of motion for momentum-driven shells (eq. [6] or eq. [25]) offers a way to investigate the question.

Even with these issues, recognizing the non-isothermal structure of real galaxies and dark-matter haloes, and working in terms of an  $M_{\text{CMO}}-V_{\text{c,pk}}$  relation, could provide a way to extend and unify discussions and analyses to include correlations between CMO masses and host-galaxy properties in systems with significant rotational support as well as (or even instead of) pressure support. This could be of particular interest in connection with nuclear star clusters

in intermediate-mass ellipticals and bulges, and even in very late-type Sc/Sd disks.

## ACKNOWLEDGMENTS

We thank Chris Power for useful discussions. We also thank the referee, Andrew King, for helpful comments. RCM is supported by an STFC studentship. The Astrophysics Group at Keele University is supported by an STFC rolling grant.

## REFERENCES

- Böker T., Laine S., van der Marel R.P., Sarzi M., Rix H.-W., Ho L.C., Shields J.C., 2002, *AJ*, 123, 1389  
 Carollo C.M., Stiavelli M., de Zeeuw P.T., Mack J., 1997, *AJ*, 114 2366  
 Côté P. et al., 2006, *ApJS*, 165, 57  
 Côté P. et al., 2007, *ApJ*, 671, 1456  
 Dehnen W., McLaughlin D.E., 2005, *MNRAS*, 363, 1057  
 Dehnen W., McLaughlin D.E., Sachania J., 2006, *MNRAS*, 369, 1688  
 Dubinski J., Carlberg R.G., 1991, *ApJ*, 378, 496  
 Fabian A.C., 1999, *MNRAS*, 308, L39  
 Ferrarese L., 2002, *ApJ*, 578, 90  
 Ferrarese L., Ford H., 2005, *Space Sci. Rev.*, 116, 523  
 Ferrarese L., Merritt D., 2000, *ApJ*, 539, L9  
 Ferrarese L. et al., 2006, *ApJ*, 644, L17  
 Gebhardt K. et al., 2000, *ApJ*, 539, L13  
 Gültekin K. et al., 2009, *ApJ* 698, 198  
 Hernquist L., 1990, *ApJ*, 356, 359  
 Ho L.C., 2007, *ApJ*, 668, 94  
 King A., 2003, *ApJ*, 596, L27  
 King A., 2005, *ApJ*, 635, L121  
 King A.R., 2010a, *MNRAS*, 402, 1516  
 King A.R., 2010b, *MNRAS*, 408, L95  
 King A.R., Pounds K.A., 2003, *MNRAS*, 345, 657  
 King A.R., Zubovas K., Power C., 2011, *MNRAS*, 415, L6  
 Kormendy J., Richstone D., 1995, *ARA&A*, 33, 581  
 Kormendy J., Bender R., 2011, *Nature*, 469, 377  
 Kormendy J., Bender R., Cornell M.E., 2011, *Nature*, 469, 374  
 McLaughlin D.E., King A.R., Nayakshin S., 2006, *ApJ*, 650, L37  
 McMillan P.J., 2011, *MNRAS*, 414, 2446  
 Murray N., Quataert E., Thompson T.A., 2005, *ApJ*, 618, 569  
 Navarro J.F., Frenk C.S., White S.D.M., 1996, *ApJ*, 462, 563  
 Navarro J.F., Frenk C.S., White S.D.M., 1997, *ApJ*, 490, 493  
 Philips A.C., Illingworth G.D., MacKenty J.W., Franx M., 1996, *AJ*, 111, 1566  
 Power C., Zubovas K., Nayakshin S., King A.R., 2011, *MNRAS*, 413, L110  
 Rossa J., van de Marel R.P., Böker T., Gerssen J., Ho L.C., Rix H.-W., Shields J.C., Walcher C.-J., 2006, *AJ*, 132, 1074  
 Silk J., Nusser A., 2010, *ApJ*, 725, 556  
 Silk J., Rees M.J., 1998, *A&A*, 331, L1

Tombesi F., Cappi M., Reeves J.N., Palumbo G.G.C.,  
 Yaqoob T., Braito V., Dadina M., 2010 A&A, 521, A57  
 Tremaine S., Gebhardt K., Bender R., Bower G., Dressler  
 A., Faber S.M., Filippenko A.V., Green R., Grillmair C.,  
 Ho L.C., Kormendy J., Lauer T.R., Magorrian J., Pinkney  
 J., Richstone D., 2002, ApJ, 574, 740  
 Volonteri M., Natarajan P., Gültekin K., 2011, ApJ, 737,  
 50  
 Wehner E.H., Harris W.E., 2006, ApJ, 644, L17

## APPENDIX A: THE MAXIMUM CRITICAL CMO MASS

Equation (35) in §4.1.3 is a general expression for the radius,  $x_{c,\max}$ , marking the onset of acceleration of the momentum-driven shell that has the maximum critical (necessary) CMO mass required to escape a non-isothermal dark-matter halo with a given mass profile  $m(x)$  and normalization  $\tilde{M}_{\text{pk}}$ :

$$\left. \frac{d \ln m}{d \ln x} \right|_{x=x_{c,\max}} = 1 + \frac{1}{2 \tilde{M}_{\text{pk}}} \frac{1}{x_{c,\max}} \left. \frac{dm}{dx} \right|_{x=x_{c,\max}}. \quad (\text{A1})$$

Once this is solved for  $x_{c,\max}$ , then equation (36) gives the value of the maximum critical CMO mass for the halo in question:

$$\tilde{M}_{\text{crit}}^{\max} = \frac{m^2(x_{c,\max})}{x_{c,\max}^2} \left[ 1 - \frac{1}{\tilde{M}_{\text{pk}}} \frac{m(x_{c,\max})}{x_{c,\max}^2} \right]^{-1}. \quad (\text{A2})$$

In the limit that  $\tilde{M}_{\text{pk}} \rightarrow \infty$ , the second term on the right-hand side of equation (A1) tends to zero, so that

$$\left. \frac{d \ln m}{d \ln x} \right|_{x=x_{c,\max}} \rightarrow 1 \quad \text{as} \quad \tilde{M}_{\text{pk}} \rightarrow \infty. \quad (\text{A3})$$

But  $m(x)$  is defined such that (see equations [23] and [24])

$$m(1) = 1 \quad \text{and} \quad \left. \frac{d \ln m}{d \ln x} \right|_{x=1} = \frac{x}{m} \left. \frac{dm}{dx} \right|_{x=1} = 1, \quad (\text{A4})$$

so we conclude that  $x_{c,\max} \rightarrow 1$  (the peak of the circular speed curve) for large halo masses  $\tilde{M}_{\text{pk}} \rightarrow \infty$ . We therefore look for the dependence of  $x_{c,\max}$ , and then  $\tilde{M}_{\text{crit}}^{\max}$ , on  $\tilde{M}_{\text{pk}}$  for large but finite  $\tilde{M}_{\text{pk}}$  (which is the observationally relevant situation; see the discussion before Figure 3 in §4.2), which also means for values of  $x_{c,\max}$  close to 1.

We define

$$m_1'' \equiv \left. \frac{d^2 m}{dx^2} \right|_{x=1}, \quad (\text{A5})$$

so expanding  $m(x)$  in a Taylor series about  $x = 1$  leads to

$$m(x) = x + \frac{1}{2} m_1'' (x-1)^2 + \mathcal{O}(x-1)^3 \quad (\text{A6})$$

$$\frac{dm}{dx} = 1 + m_1'' (x-1) + \mathcal{O}(x-1)^2 \quad (\text{A7})$$

$$\left. \frac{d \ln m}{d \ln x} \right|_{x=x_{c,\max}} = 1 + m_1'' (x_{c,\max} - 1) + \mathcal{O}(x_{c,\max} - 1)^2, \quad (\text{A8})$$

where we have again used the facts (in equation [A4]) that  $m = 1$  and  $dm/dx = 1$  at  $x = 1$  always. Equation (A1) in the limit  $|x_{c,\max} - 1| \ll 1$  is then

$$(x_{c,\max} - 1) \left[ m_1'' - \frac{1}{2 \tilde{M}_{\text{pk}}} (m_1'' - 1) \right]$$

$$= \frac{1}{2 \tilde{M}_{\text{pk}}} + \mathcal{O}(x_{c,\max} - 1)^2 \quad (\text{A9})$$

Since the limit  $x_{c,\max} \rightarrow 1$  corresponds to  $\tilde{M}_{\text{pk}} \rightarrow \infty$ , terms in  $(x_{c,\max} - 1)/\tilde{M}_{\text{pk}}$  are of the same order as terms in  $(x_{c,\max} - 1)^2$  or terms in  $1/\tilde{M}_{\text{pk}}^2$ . With this in mind, solving equation (A9) for  $x_{c,\max}$  as a function of  $\tilde{M}_{\text{pk}}$  gives

$$x_{c,\max} = 1 + \frac{1}{2 m_1''} \frac{1}{\tilde{M}_{\text{pk}}} + \mathcal{O}\left(\frac{1}{\tilde{M}_{\text{pk}}^2}\right). \quad (\tilde{M}_{\text{pk}} \gg 1) \quad (\text{A10})$$

Finally, putting this into equation (A2) yields

$$\tilde{M}_{\text{crit}}^{\max} = 1 + \frac{1}{\tilde{M}_{\text{pk}}} + \mathcal{O}\left(\frac{1}{\tilde{M}_{\text{pk}}^2}\right). \quad (\tilde{M}_{\text{pk}} \gg 1) \quad (\text{A11})$$

As discussed further in §4, this is the CMO mass that is *sufficient* to ensure the escape of *any* momentum-driven shell in *any* non-isothermal halo that has a well-defined peak in its circular-speed curve. In general, it is larger than the CMO mass that is *necessary* for the escape of any particular shell.